Performance Evaluation of Multiuser Detectors with V-BLAST to MIMO Channel

Mincheol Park

Thesis submitted to the faculty of the
Virginia Polytechnic Institute and State University
in partial fulfillment of the requirements for the degree of

Master of Science
in
Electrical Engineering

Brian D. Woerner, Chair
William H. Tranter
Jeffrey H. Reed

May 2003
Blacksburg, Virginia

Keywords: MIMO channels, BLAST, Multiuser receiver.

Performance Evaluation of Multiuser Detectors with V-BLAST to MIMO Channel

by

Mincheol Park

Committee Chairman: Dr. Brian D. Woerner

Abstract

In this thesis, we evaluate the performance of multi-user detectors over an uplink using AWGN, Rayleigh flat fading single-input single-output (SISO) and multiple-input multiple-output (MIMO) channel models. First, we review the performance of three multiuser receivers; the decorrelator, the MMSE receiver and the multistage parallel interference cancellation receiver in an AWGN and Rayleigh flat fading SISO channel. Next, the V-BLAST algorithm is reviewed and the error propagation of this algorithm is investigated. Then, the V-BLAST algorithm is combined with multiuser receivers to achieve high channel capacity while sharing the spectral resources over a MIMO channel. A bias reduction technique is considered for multistage parallel interference cancellation receiver on both SISO and MIMO channel. Finally, the effect of channel estimation error and timing delay estimation error is evaluated for MIMO systems with multiple users.

Acknowledgements

I would like to express thanks to my advisor Dr. Brian D. Woerner for his invaluable advice and comments from deciding the thesis topic to revising the writing. His guidance and consistent encouragement allowed me complete this work. I am extremely impressed with his teaching, advising and generosity. I am deeply grateful to Dr. William H. Tranter and Dr. Jeffrey H. Reed for accepting to be on my thesis committee and for providing advice in and out of class. Thanks to Haesoo Kim and Kyehun Lee for helpful discussion and comments. I appreciate other VT faculty members, staffs and colleagues. Finally, I thank my parents for their support and endless love through my life.

Contents

List of Figures

Chapter 1

Introduction

1.1 MIMO Channel

Techniques that use arrays of multiple transmit and receive antennas may offer high capacity to present and future wireless communications systems, which place severe demands on current spectral resources. Multiple-input multiple-output (MIMO) systems provide for a linear increase of capacity with the number of antenna elements, affording significant increases over single-input single-output (SISO) systems. To evaluate the performance of MIMO systems, the MIMO channel must be appropriately modeled. It is common to model the MIMO channel assuming an independent quasi-static flat Rayleigh fading at all antenna components. There are various schemes that can be applied to MIMO systems such as space time block codes [1] [2], space time trellis codes [3] and Bell-Labs Layered Space Time architecture [4]. With a simple MIMO channel system consisting of n_T transmit antennas and n_R receive antennas, the channel matrix is described as

$$H = \begin{pmatrix} h_{11} & \cdots & h_{1n_T} \\ \vdots & \ddots & \vdots \\ h_{n_R 1} & \cdots & h_{n_R n_T} \end{pmatrix}, \tag{1.1}$$

where

$$h_{ij} = \alpha + j\beta \tag{1.2}$$

$$= \sqrt{\alpha^2 + \beta^2}\; e^{-j\arctan\frac{\beta}{\alpha}}$$

$$= \left| h_{ij} \right| e^{j\phi_{ij}} \quad .$$

In a rich scattering environment without line-of-sight, the path gains $\left| h_{ij} \right|$ as shown in Figure 1.1 from j transmit antenna to i receive antenna are Rayleigh distributed. These path gains are modeled with zero mean and 0.5 variance independent complex Gaussian random variables per dimension. The channel characteristics are not changed during the transmission period of an entire frame in accordance with the quasi-static flat fading assumption. The spatial separation of antenna elements is large enough to lead to independent channel effect.

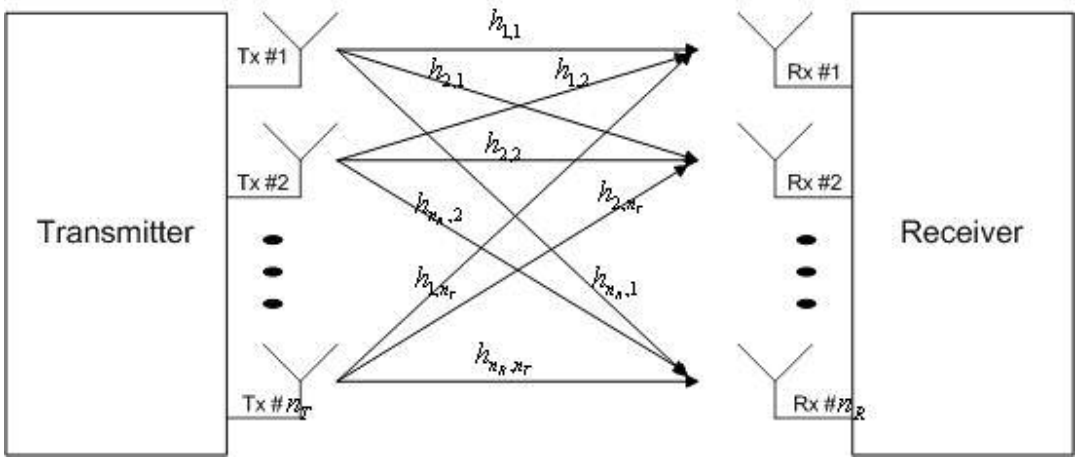

Figure 1.1 Illustration of MIMO channel

1.2 Direct Sequence Spread Spectrum

MIMO channels for single users have been investigated. We want to investigate the multiple access characteristics of MIMO channels. One means of creating multiple access capability in DS-SS, which supplies CDMA. There are many ways to generate spread spectrum signals [5] such as direct sequence (DS), frequency hop (FH), time hop (TH) and multi-carrier (MC). Of course, one can also mix these spread spectrum techniques to form hybrids that have the advantages of different

techniques. Spread spectrum systems were originally developed in response to the hostile communications environments faced by military communications systems, but have also found a wide range of commercial applications, including both cellular telephone and wireless local area networks.

One way of spreading the spectrum of the transmitted signal is to modulate the data signal by high rate pseudo-random sequences, such as Walsh codes, m-sequences, Gold sequences or Kasami sequences, before the mixing the signal up to the carrier frequency for transmission. This spreading method is called direct sequence spread spectrum (DS-SS). Figure 1.2 shows the spectra of signals before and after direct sequence spreading. The spreading technique increases the bandwidth due to the increase in the symbol rate as shown in Figure 1.2.

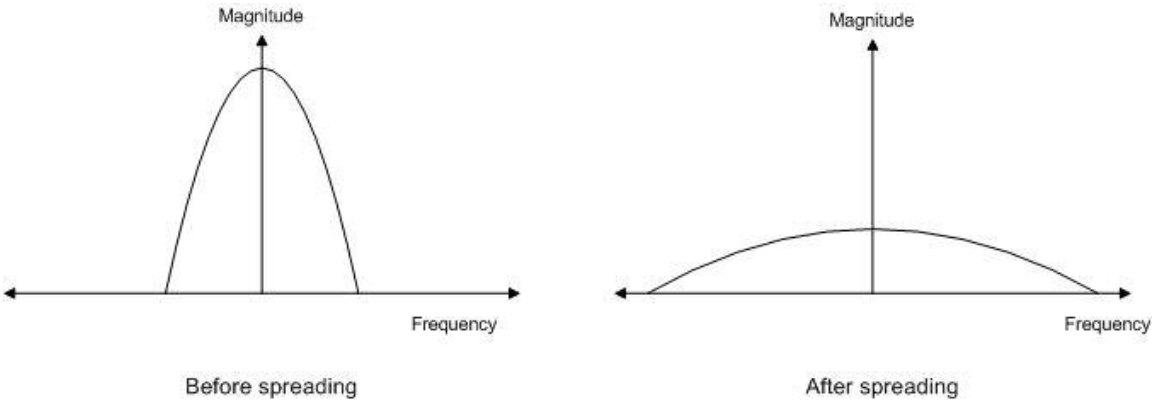

Figure 1.2 Spectra of signal before and after direct sequence spreading

1.3 Purposes and Outline of Contents

The purpose of this thesis is to compare the performance of several multiuser receivers combined with V-BLAST for uplink SISO and MIMO systems. The thesis is organized as follows.

Chapter 1 provides a brief introduction of MIMO channel model, spread spectrum and outline of the

rest of the thesis.

In Chapter 2 a simple multiuser uplink system model is introduced. Linear and non-linear multiuser receivers for a SISO channel are presented and their performance is investigated with perfect knowledge of channel and timing delay under both AWGN and Rayleigh fading channel conditions. A bias reduction technique for multistage parallel interference cancellation receiver is reviewed.

In Chapter 3 the architecture of Vertical Bell-Labs Layered Space Time architecture (V-BLAST) is presented. A system with four transmit and four receive antennas is consider for simulation. The performance of parallel interference cancellation (PIC) and successive interference cancellation (SIC) is compared based on zero-forcing (ZF) nulling and minimum mean squared error (MMSE) criteria. The effect of error propagation is shown for the case of both PIC and SIC.

In Chapter 4 a multiuser detection scheme is combined with V-BLAST within MIMO system. Extended receiver structures for MIMO are illustrated and their performances are analyzed. The simulation is executed with assumption of perfect knowledge of channel and timing delay. It is verified that the performance of multistage parallel interference cancellation receiver combined with V-BLAST is highly degraded at uplink MIMO due to the interference from multiple transmit antennas.

In Chapter 5 the effect of imperfect channel estimation and timing delay estimation error is investigated for both MIMO and SISO channels.

Finally in Chapter 6, a summary of the results is presented and the some ideas for future work are provided.

1.3 Contributions

The contributions of this thesis include:

- A combined VBLAST decoding algorithm, which employs successive interference cancellation at the first step, followed by parallel interference cancellation (PIC) as a second step, is introduced. The performance of this combined scheme is investigated and it is verified that the combined scheme exploits both the advantages of ordering and of the PIC algorithm.
- A mathematical formulation for multi-user V-BLAST receivers operating in MIMO channels is developed.
- Linear and non-linear receiver structures are described for a VBLAST system with multiple asynchronous users. The performance of these receiver structures is evaluated using a simulation model.
- The effect of channel estimation error and delay estimation error are investigated for VBLAST receivers in both SISO and MIMO channels.

Chapter 2

Multi-user Detection for SISO Channels

In wireless communication, several techniques such as Time Division Multiple Access (TDMA), Frequency Division Multiple Access (FDMA) and Code Division Multiple Access (CDMA) are used for sharing the spectrum resources available for use. TDMA assigns different time slots to users while FDMA assigns a different frequency to each user. However, the CDMA technique shares the entire bandwidth by distinguishing signals with a unique signature for each user. A promising technique to achieve improved capacity for CDMA is multi-user detection [6]. A conventional receiver, that is a matched filter receiver, does not perform well when the desired signal is subjected to strong interference from other signals. Specially, the reverse link from a mobile to a base station leads to strong multiple access interference since synchronism between users is lacking, thus perfectly uncorrelated sequences cannot be generated for reverse link [7]. In this chapter, we compare the performance of four multiuser receivers for the reverse link of a wireless network. The four receivers of interest are the conventional [6], the decorrelating [8], the minimum mean squared error (MMSE) [6] and multistage parallel interference cancellation (MPIC) receiver [9]. Gold sequences with length 31 are used in the simulation as the signatures of each user. In Section 2.1, the system model [7] [10] is illustrated for an AWGN channel, Section 2.2 reviews multiuser receivers, Section 3.3 describes the simulation conditions and discusses the results under for both an AWGN channel and a Rayleigh fading channel.

2.1 System Model

The received baseband signal $r(t)$, where $s_k(t)$ is the transmitted signal for the k^{th} user, from K users is formulated as follows:

$$r(t) = \sum_{k=1}^{K} h^k s_k(t-\tau_k) + n(t) \tag{2.1}$$

$$s_k(t-\tau_k) = \sqrt{P_k} b_k(t-\tau_k) c_k(t-\tau_k) e^{j\theta_k}, \tag{2.2}$$

where P_k is the k^{th} user's received signal power, $c_k(t)$ represents the k^{th} users spreading sequence, $b_k(t)$ represents the k^{th} users polar data signal, τ_k represents a time delay for the k^{th} user that accounts for the asynchronous nature of the reverse link, θ_k is the received phase of the k^{th} user relative to an arbitrary reference phase and h^k represents the fading channel coefficient and phase in complex form. The fading coefficients are modeled with an independent zero mean complex Gaussian random variable with variance 0.5 per dimension. We can ignore the h^k term when considering AWGN channel. $n(t)$ represents the additive white Gaussian noise. Figure 2.1 illustrates the system defined by with Eq. (2.1) and (2.2).

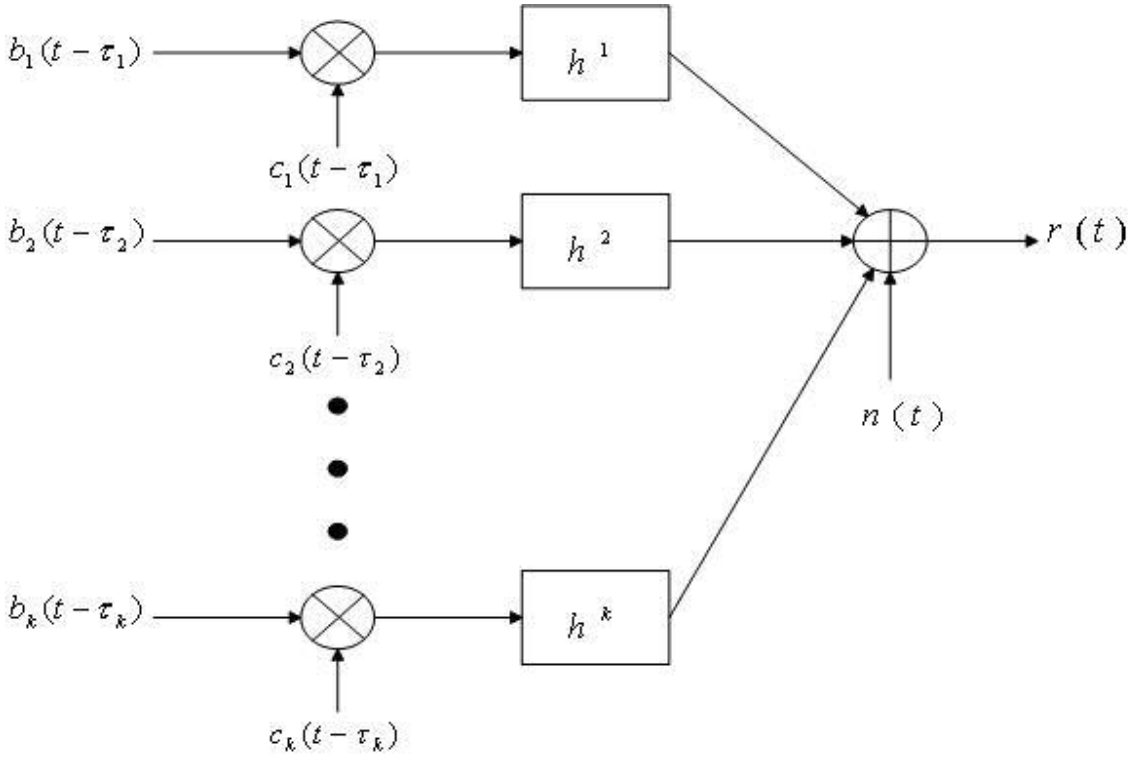

Figure 2.1 Multi-user System Model on SISO channels

2.2 Multi-user Receivers

2.2.1 Conventional Receiver

The sufficient statistics for determining the transmitted symbols b can be shown to be the matched filter output y that results from correlation with each users spreading sequence. The vector form of sufficient statistics [6] may be represented as

$$\mathrm{y} = RW\mathrm{b} + \mathrm{n}, \tag{2.3}$$

where R is a correlation matrix with size $KN_f \times KN_f$.

$$R = \begin{pmatrix} \mathrm{R}(0) & \mathrm{R}(-1) & 0 & \cdots & 0 \\ \mathrm{R}(1) & \mathrm{R}(0) & \mathrm{R}(-1) & & \vdots \\ 0 & \mathrm{R}(1) & \mathrm{R}(0) & \ddots & \\ \vdots & \vdots & \vdots & \ddots & \mathrm{R}(-1) \\ 0 & \cdots & 0 & \mathrm{R}(1) & \mathrm{R}(0) \end{pmatrix} \tag{2.4}$$

The element of $\mathrm{R}(i)$ with dimensions $K \times K$ is defined by

$$\rho_{l,m}(i) = \int_{-\infty}^{\infty} c_l(t-\tau_l)\, c_m(t+iT-\tau_m)dt\,, \tag{2.5}$$

where T is the symbol duration. W represents the $KN_f \times KN_f$ diagonal matrix of the square root of user received energies and b is the KN_f length vector form of all user's data symbols where each element corresponds to a data symbol. K denotes the number of active users and N_f represents the size of consecutive transmitted symbols or frame size.

The decision metric for conventional receiver is

$$\hat{\mathrm{b}} = \mathrm{sgn}[\mathrm{y}] = \mathrm{sgn}[RW\mathrm{b} + \mathrm{n}]. \tag{2.6}$$

We observe that the correlation matrix affects the decision of transmitted symbols. That is, the conventional detector is vulnerable to interference from other users especially in an asynchronous system, because it is not possible to design the signature sequences for any pair of users that are orthogonal for all time offsets. Therefore, interference from other users is unavoidable in an asynchronous system with a conventional detector.

2.2.2 Decorrelating Receiver

A linear detector is a detector with decision metric

$$\hat{\mathrm{b}} = \mathrm{sgn}[\mathrm{Ty}] \ , \tag{2.7}$$

where T is a linear transformation of the sufficient statistics. The conventional receiver has $\mathrm{T} = I$, which is an identity matrix as shown in previous section.

Similarly, the decorrelating receiver has $\mathrm{T} = R^{-1}$ [6][8]. Therefore, the estimated symbols are expressed by

$$\hat{\mathrm{b}} = \mathrm{sgn}[W\,\mathrm{b} + R^{-1}\mathrm{n}] \ , \tag{2.8}$$

assuming perfect knowledge of phase and time delay.

The linear transformation T is derived from the maximization of the likelihood function or the minimization of the cost function Eq (2.9):

$$\Lambda(\mathrm{b}) = (\mathrm{y} - R\mathrm{b})^T R^{-1}(\mathrm{y} - R\mathrm{b}) . \tag{2.9}$$

The best linear estimate of b is

$$\mathrm{b}_{\mathrm{est}} = R^{-1}\mathrm{y} \ . \tag{2.10}$$

The detected symbols in (2.8) are obtained by taking the sign of each element of $\mathrm{b}_{\mathrm{est}}$.

2.2.3 MMSE Receiver

Another type of linear detector can be obtained if a linear transformation is sought which minimizes the mean squared error between the transmitted symbols and the outputs of the transformation $E\{(\mathrm{b} - T\mathrm{y})^T(\mathrm{b} - T\mathrm{y})\}$. In this case, the linear transformation of the decorrelating receiver used in previous section is replaced by $\mathrm{T} = (R + N_0 / 2W^2)^{-1}$ for the MMSE receiver [6]. In this case, we recognize that the performance of the MMSE receiver approaches that of the decorrelating receiver as N_0 goes to zero. The MMSE detector seeks to balance between cancellation of the interference

and reduction of noise enhancement. Therefore, the MMSE receiver outperforms the decorrelator at low SNR while the performance of MMSE receiver approaches that of decorrelator at high SNR. However, estimation of SNR at the receiver is often required for obtaining the benefit of a MMSE receiver so additional implementation effort is necessary.

2.2.4 Multistage Parallel Interference Cancellation

The multistage interference cancellation technique was first proposed in [11] and developed in [9]. Multistage receivers have multiple stages of interference cancellation. This technique can be combined with the concept of parallel interference cancellation. At each stage of MPIC, any receiver can be used but the accuracy of the first stage or previous stage affects the performance of the whole receiver. In this section, a conventional receiver is considered as a first stage to estimate the channel gain and data symbol. The estimates for each user are used to eliminate the interference of the other user's signal by subtracting the interferer from the desired signal. The interference cancellation depends on the accuracy of estimates at the previous stage. Since the inaccurate estimates lead to imperfect interference cancellation in real system, several stages can be used or a more powerful estimate technique such as a channel coding scheme can be utilized to overcome this imperfection. In addition, an improved MPIC scheme with partial cancellation at each stage is introduced to mitigate bias in the decision statistics of MPIC [12].

The MPIC decision metric for S-stage parallel cancellation scheme is represented as

$$\hat{b} = \mathrm{sgn}[y^{(s)}] \ , \tag{2.11}$$

where

$$y_k^{(s)} = \frac{1}{T}\int r_k^{(s)}(t)\ c_k(t-\hat{\tau}_k)\ dt, \tag{2.12}$$

$$r_k^{(s)}(t) = r(t) - \sum_{j\neq k} y_j^{(s-1)}\ c_j(t-\hat{\tau}_j)\ . \tag{2.13}$$

$r_k^{(s)}$ is the S stage signal of the k^{th} user after cancellation and $\hat{\tau}_k$ represents the estimated time delay of k^{th} user. The bias increases linearly with system loading [12] such that the bias affects the decision statistics especially in first stage of interference cancellation. On proceeding subsequent stages, the effect of bias is minimal. The proposed method [12] to reduce the influence of bias is to adopt a partial-cancellation factor $C^{(s)}$ as follows:

$$r_k^{(s)}(t) = r(t) - C^{(s)}\sum_{j\neq k} y_j^{(s-1)}\ c_j(t-\hat{\tau}_j) \tag{2.14}$$

This factor is assigned a value at every stage in the range [0,1].

2.3 Simulation Results

In this section, we compare the performance of four multiuser detectors for both AWGN and Rayleigh fading channels. For the simulation, we assumed perfect power control, channel estimation and time delay estimation. Gold sequences [13] are generated with processing gain 31. Five samples per chip were used in the simulation. Time delays are generated randomly for an asynchronous system. The fading channel is static during the 20 symbols that constitute one frame.

2.3.1 AWGN Channel

Figure 2.2 depicts the influence of various partial-cancellation factors for an AWGN channel. Five values at the range of [0,1] are selected for simulation simplicity and a three-stage PIC receiver is

considered. In this simulation result, we observe that partial-cancellation factors of 0.5 and 0.7 at second stage are good choices for a three-stage parallel interference cancellation receiver. The performance of those receivers with 0.5 and 0.7 partial-cancellation factor is almost equivalent.The three-stage PIC with 0.5 partial factor outperforms slightly the three-stage PIC with 0.7 partial factor for a highly loaded system, whereas for a lightly loaded system the receiver with 0.7 partial factor is slightly better than receiver with 0.5 partial factor.

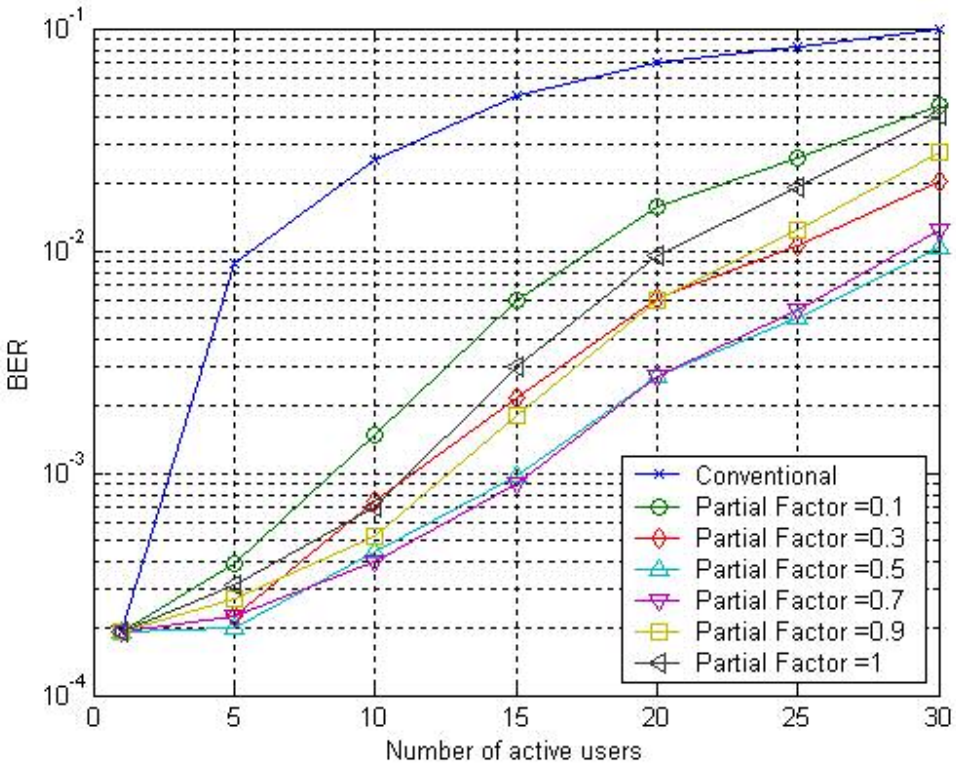

Figure 2.2 BER versus number of users for various partial cancellation factors for MPIC in an AWGN channel with QPSK modulation, $E_b / N_o = 8dB$, Gold sequences, and a processing gain of 31.

Figure 2.3 shows the capacity for an AWGN channel with perfect power control, perfect channel estimation and perfect time delay estimation. Two types of MPIC receivers are simulated. One is a three-stage PIC receiver with a matched filter receiver at the first stage. The other is a two-stage PIC receiver with a decorrelator at the first stage. Partial interference cancellation is used for three-stage PIC with a partial cancellation factor of 0.5 at the second stage. We observe that the performance of the MPIC receiver depends on the accuracy of the first stage or previous stage by comparing the performance with the two-stage PIC with decorrelator at the first stage to the three-stage PIC with matched filter receiver at the first stage. This is true even if the three-stage PIC receiver with a matched filter at the first stage performs the interference cancellation at one more stage compared to the two-stage PIC receiver. The more accurate detection of the decorrelator cancelling the multiuser access interference contributes to the MPIC receiver performance at following stage. Moreover, the performance of MPIC receiver is improved as the number of stages of cancellation at receiver grows large. The MMSE receiver slightly outperforms decorrelator. The improvement becomes larger on highly loaded system. Figure 2.4 illustrates the performance of multiuser receivers for a system with 10 users. The MPIC receiver provides slightly superior performance compared to the linear detectors.

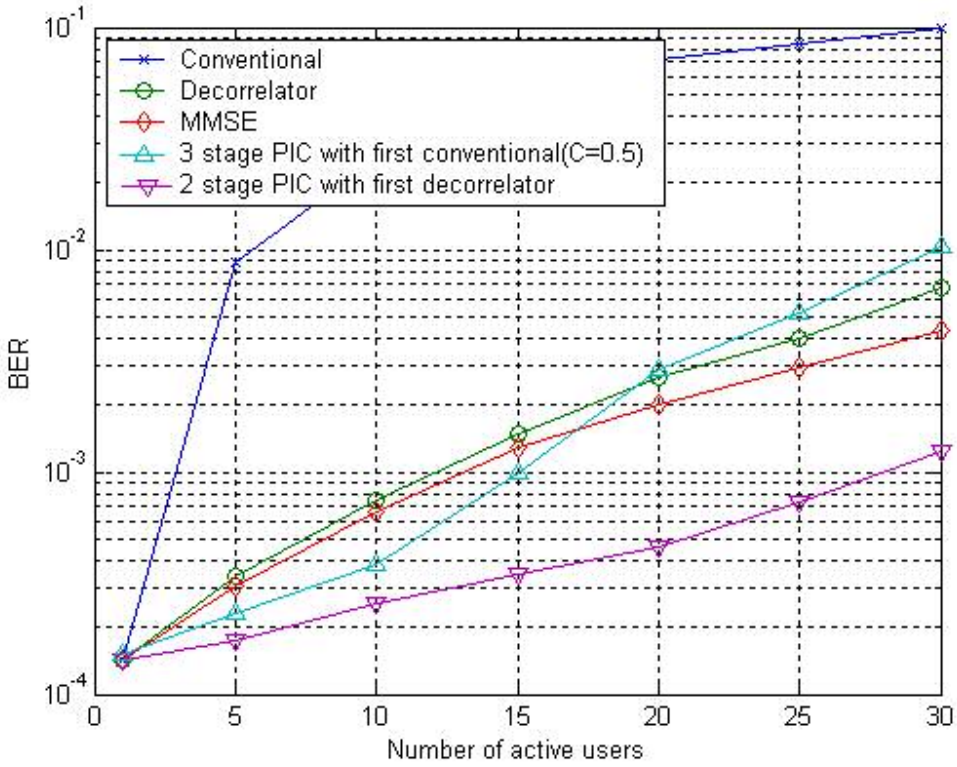

Figure 2.3 BER versus number of users for perfect estimation of time delay and channel in an AWGN channel, with QPSK modulation, $E_b / N_o = 8dB$, Gold sequences, and a processing gain of 31.

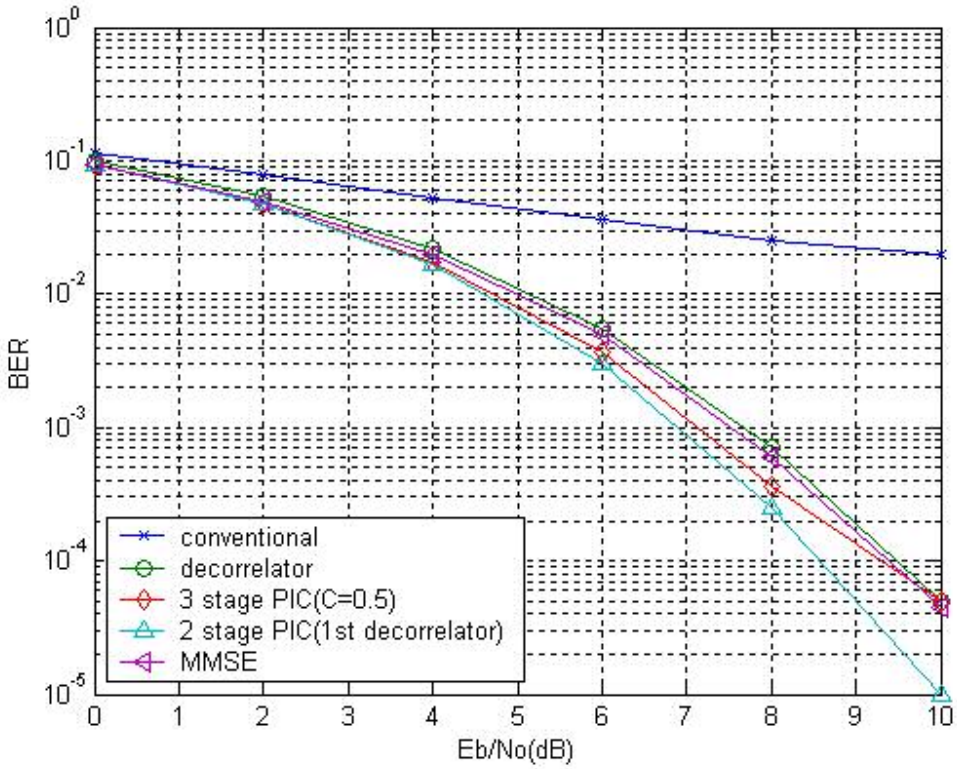

Figure 2.4 BER versus Eb/No with perfect channel estimation and perfect time delay estimation in an AWGN channel with QPSK modulation, Gold sequences with a processing gain of 31.

2.3.1 Rayleigh Flat Fading Channel

The performance of a 3-stage PIC receiver in terms of different value of partial-cancellation factor at the second stage with perfect knowledge of channel is presented in Figure 2.5. The channel is assumed to be flat with a single path channel experiencing Rayleigh fading. The average E_b / N_o is fixed at 20 dB. This simulation result shows that the partial-cancellation factor of 0.7 is the best choice for this system.

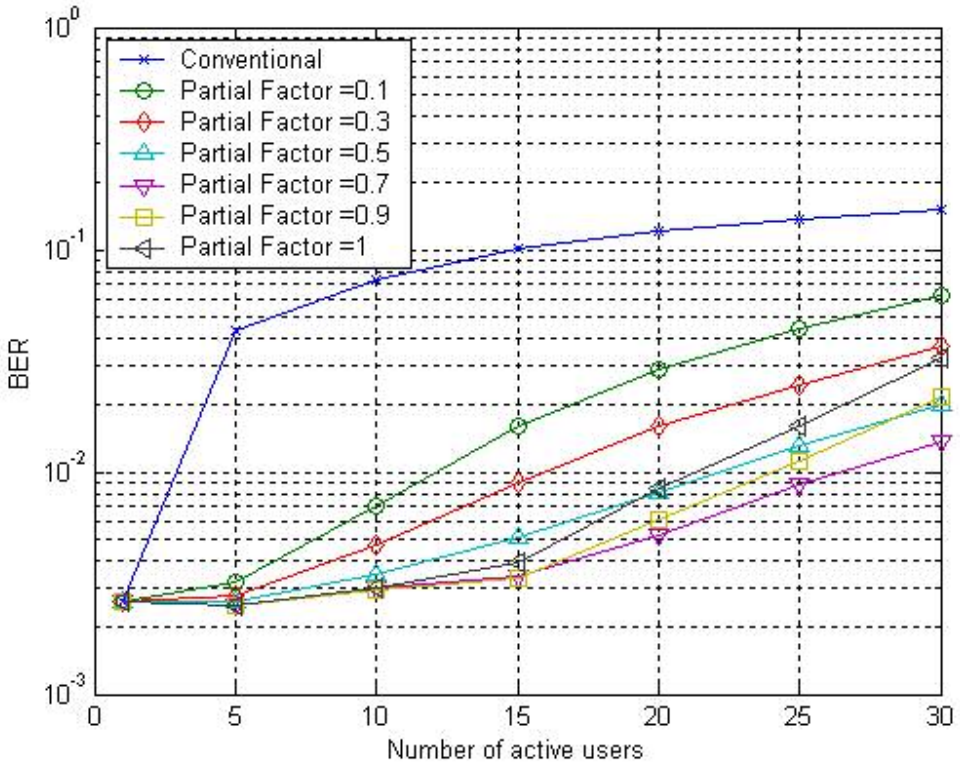

Figure 2.5 BER versus number of users for various partial cancellation factors for MPIC in a flat fading SISO channel with QPSK modulation, $E_b / N_o = 20dB$, Gold sequences with a processing gain of 31.

As shown in Figure 2.6 and Figure 2.7, the decorrelator, MMSE receiver and MPIC receiver give the significant improvement over the conventional receiver. The decorrelator and MMSE receiver are equivalent in terms of performance in a flat fading SISO channel unlike for an AWGN channel. The performance of three-stage PIC is equivalent with that of the decorrelator or the MMSE receiver in lightly loaded systems with fewer than 10 active users, whereas the performance is highly degraded as the number of active users increases. The amount of degradation for fading

channels is larger than for the AWGN channel.

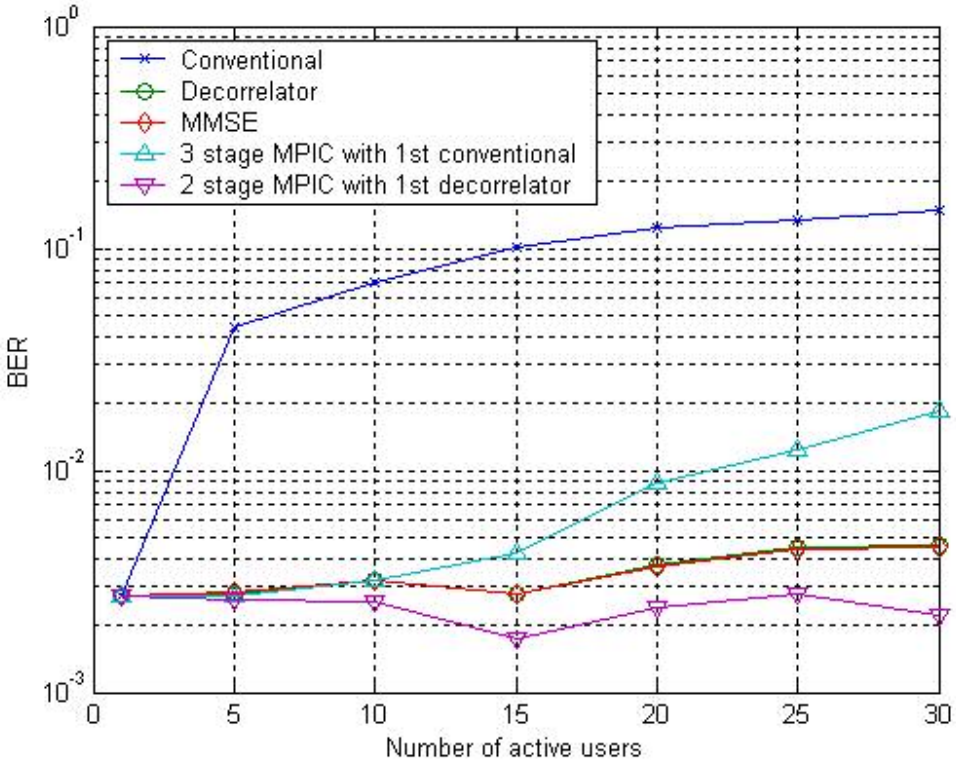

Figure 2.6 BER versus number of users with perfect estimation of time delay and channel at a Flat fading SISO channel with QPSK modulation, $E_b / N_o = 20dB$, Gold sequences with a processing gain of 31.

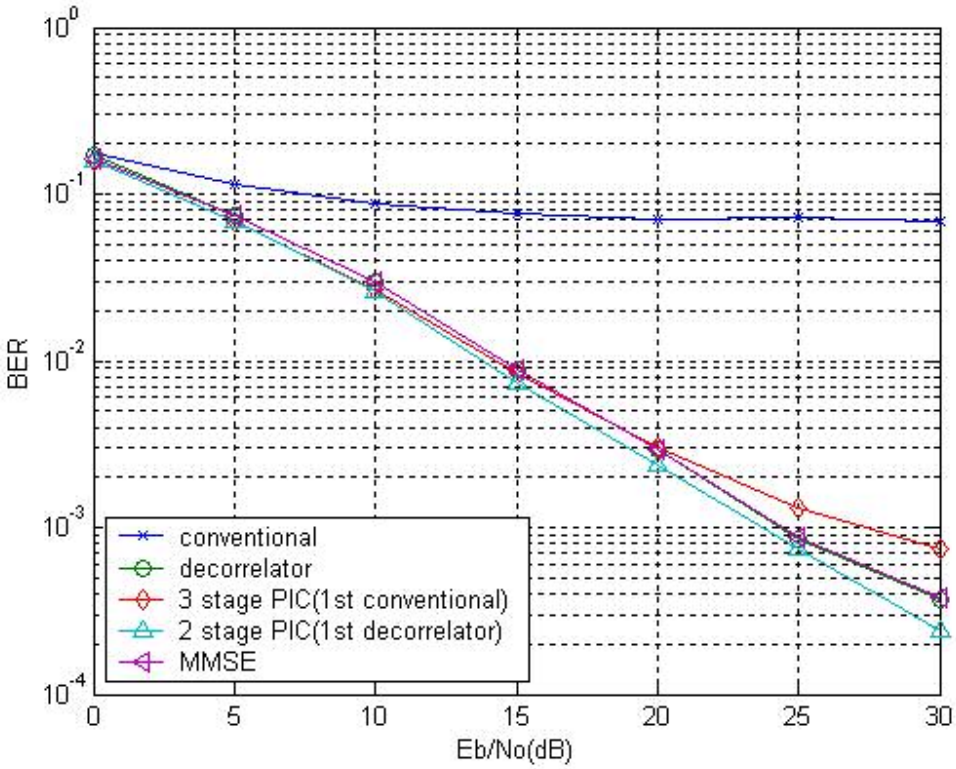

Figure 2.7 BER curves with perfect channel estimation and perfect time delay estimation in a Flat fading SISO channel with QPSK modulation, Gold sequences with a processing gain of 31.

2.4 Chapter Summary

In this chapter, four types of multiuser detectors were introduced. We characterized the performance of these receivers, such as conventional, decorrelator, MMSE and MPIC, for AWGN and Rayleigh flat fading channels assuming perfect estimation of phase and timing delay. In the case of MPIC, we verified performance gain from using the partial-cancellation factor for both AWGN and Rayleigh flat fading channels. These results are all well known from the previous literature. Our goal here was to establish a performance baseline so that these results could be compared with performance of

multi-user systems in MIMO channels. In the next chapter, we turn to that subject.

Chapter 3

Vertical Bell Labs Layered Space-Time Architecture

Flat fading MIMO (Multiple Input and Multiple Output) channels having multiple transmit and receive antennas were shown to offer relatively huge spectral efficiencies compared to SISO (Single Input and Single Output) channels [14][15]. Capacity increases linearly with the number of transmit antennas as long as the number of receive antennas is greater than or equal to the number of transmit antennas. To achieve this capacity, Diagonal BLAST was proposed by Foschini [15]. This scheme utilizes multi-element antenna arrays at both ends of wireless link. However, the complexities of D-BLAST implementation led to V-BLAST which is a modified version of BLAST [16]. Two nulling criteria, namely Zero-Forcing (ZF) [17] and Minimum Mean Squared Error (MMSE) [10], are utilized as detection algorithms. Originally, the BLAST detection scheme was based on a successive interference cancellation [16] [17] [18]. A parallel interference cancellation scheme was also proposed later [19].

BLAST detectors including both SIC and PIC suffer from the error propagation problem, so that they lead to the poor energy efficiency which can be improved if the previously detected layers were perfectly cancelled because the following layers depend highly on the result of the previous detected signals. The error propagation problem of BLAST detectors can be reduced with channel coding and interleaving [20] [21].

In this chapter, we verify the error propagation problem of BLAST detectors and compare the performance of PIC and SIC. Section 3.1 describes V-BLAST architecture and simulation procedures. Section 3.2 reviews the principles of BLAST based on both PIC and SIC. In Section 3.3, we investigate the error propagation problem.

3.1 V-BLAST Architecture

The V-BLAST high-level block diagram is illustrated in Figure 3.1. The received vector with size $n_R \times 1$ is modeled by [16]

$$r = H\ a + n\ , \tag{3.1}$$

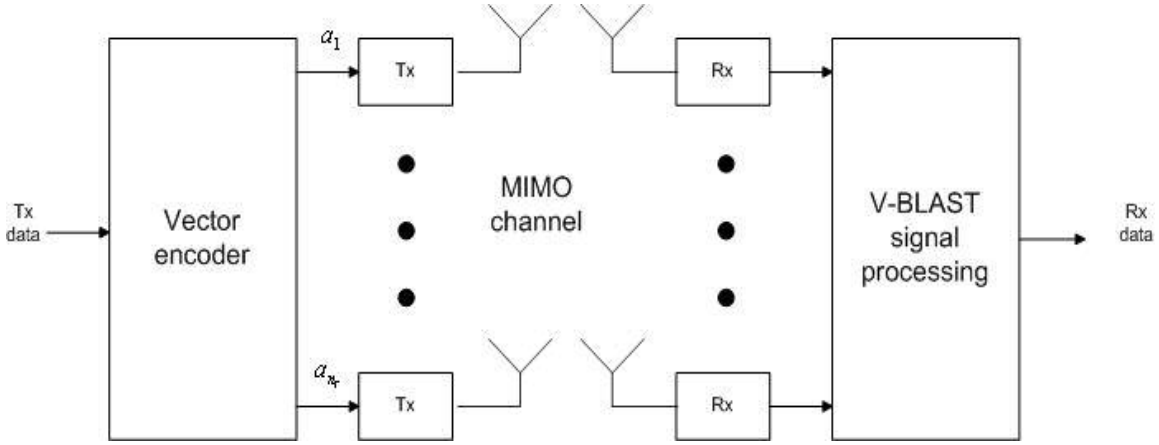

Figure 3.1 V-BLAST system diagram

where H represents the channel matrix with dimension $n_R \times n_T$, whose element $h_{i,j}$ represenst the complex fading coefficient for the path from transmit j to receive antenna i. These fading coefficients are modeled by an independent zero mean complex Gaussian random variable with

variance 0.5 per dimension. a denotes the vector of transmitted symbols with dimension $n_T \times 1$, n represents a complex vector of independent samples of AWGN over each received antenna with zero mean and variance σ_n^2.

The nulling matrix G is described in Eq. (3.2) and (3.3) for the ZF and MMSE criteria with the form of pseudo-inverse of the channel matrix H:

$$G = (H^+ H)^{-1} H^+ \tag{3.2}$$

$$G = (H^+ H + \frac{\sigma_n^2}{\sigma_d^2})^{-1} H^+, \tag{3.3}$$

where $\frac{\sigma_n^2}{\sigma_d^2}$ denotes the inverse of signal-to-noise ratio at each receive antenna. H^+ represents the conjugate transpose matrix of channel matrix H.

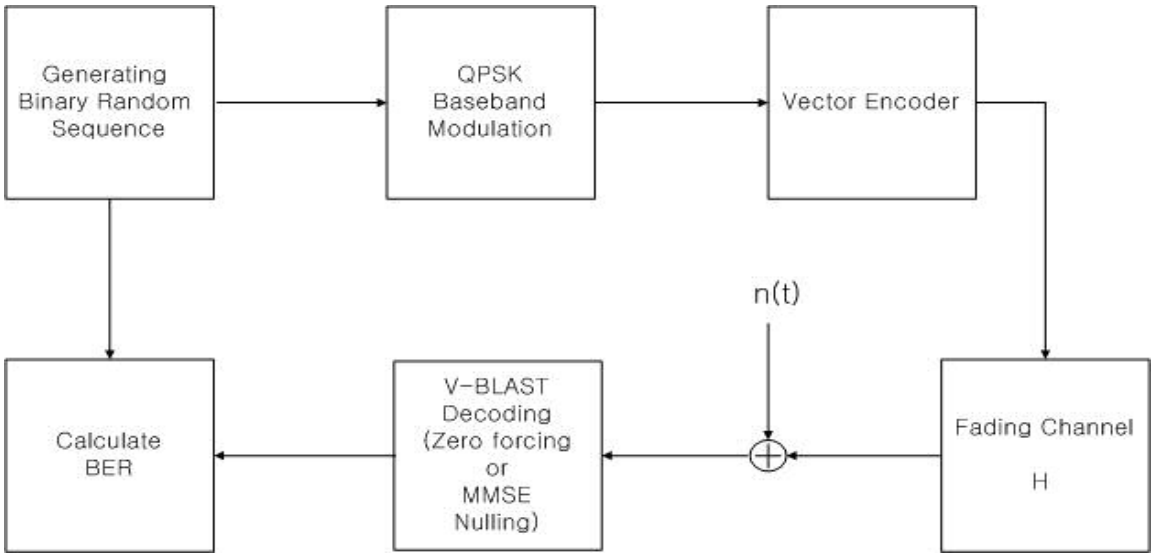

Figure 3.2 Simulation Block Diagram for V-BLAST

Figure 3.2 describes simulation block diagram for V-BLAST scheme.

To decode the transmitted symbols of the first layer, the receiver needs to estimate the channel

matrix using pilots. In this simulation, the fading channel characteristics are assumed to be known perfectly at the receiver. The transmitter consists of a binary random generator, a QPSK baseband modulator and a vector encoder. The binary random generator generates the transmitted bits. These bits are modulated in the QPSK modulator using the complex envelope form. It is assumed that each symbol has an ideal rectangular pulse shape and may be sampled with a single point per symbol. The vector encoder maps the symbols to each antenna. In the channel block, the transmitted symbols undergo Rayleigh fading and additive noise. Rayleigh fading channel coefficients are generated with two independent Gaussian random variables with unit variance. The phase delay is distributed uniformly between $-\pi$ and π. In addition, the channel is assumed to be quasi-stationary, that is, the channel coefficients do not vary during the given period time. The receiver is made up of decoding processing and an error rate calculation block. At the decoding processing block, we simulate the several types of schemes reviewed briefly in analysis section. The decoding methods are reviewed in the following section. PIC does not need to consider the ordering issue since it cancels out all other paths' interference in the same stage.

We compare the performance for ordered and non-ordered systems, and the simple ZF and MMSE technique are compared on the basis of PIC and SIC algorithm. For applying the MMSE technique, we need to know the SNR at the receiver. Therefore, knowledge of the SNR is also assumed at the receiver. Finally the SER is calculated by comparing the originally transmitted symbols with received symbols that are estimated at the receiver.

3.2 Comparison of SIC and PIC

3.2.1 Successive Interference Cancellation

The SIC detection algorithm operates by successively canceling out one layer per iteration. The ordering of detected layers gives effect to the performance of the SIC detector. The algorithm is shown in [17]. The nulling matrix is first initialized with Eq. (3.2) and (3.3) for ZF and MMSE criteria respectively by assuming perfect channel estimation. For the ordering scheme, we determine the biggest post-detection signal-to-noise ratio. This corresponds to choosing the minimum norm row of the nulling matrix G in each iteration. First the layered signal is decoded with row vector of G suppressing the signals from all other antennas shown in Eq. (3.4). The received signal after i^{th} layer interference cancellation is formulated by

$$r_{i+1} = r_i - \tilde{a}_i (H)_i , \tag{3.4}$$

where $\tilde{a}_i$ is the decoded symbols in the i step. $(H)_i$ is the i^{th} column of channel matrix. G is newly updated by nulling out the previous pseudo-inverse of the channel matrix. This procedure is repeated until symbols from all transmit antennas are decoded in a similar manner. The non-ordered scheme does not need to determine the largest post-detection SNR but chooses the row vector of nulling matrix randomly.

The performance of the SIC detector for V-BLAST is shown in Figure 3.3. We can observe that the ordering of layers improves performance considerably. The ordering scheme obtains about 3 dB and 8 dB performance gain compared with non-ordering scheme at target BER 10^{-3} based on ZF and MMSE nulling criterion respectively. In addition, MMSE nulling criteria outperforms ZF, even if both of them suffer from poor energy efficiency caused by error propagation problem.

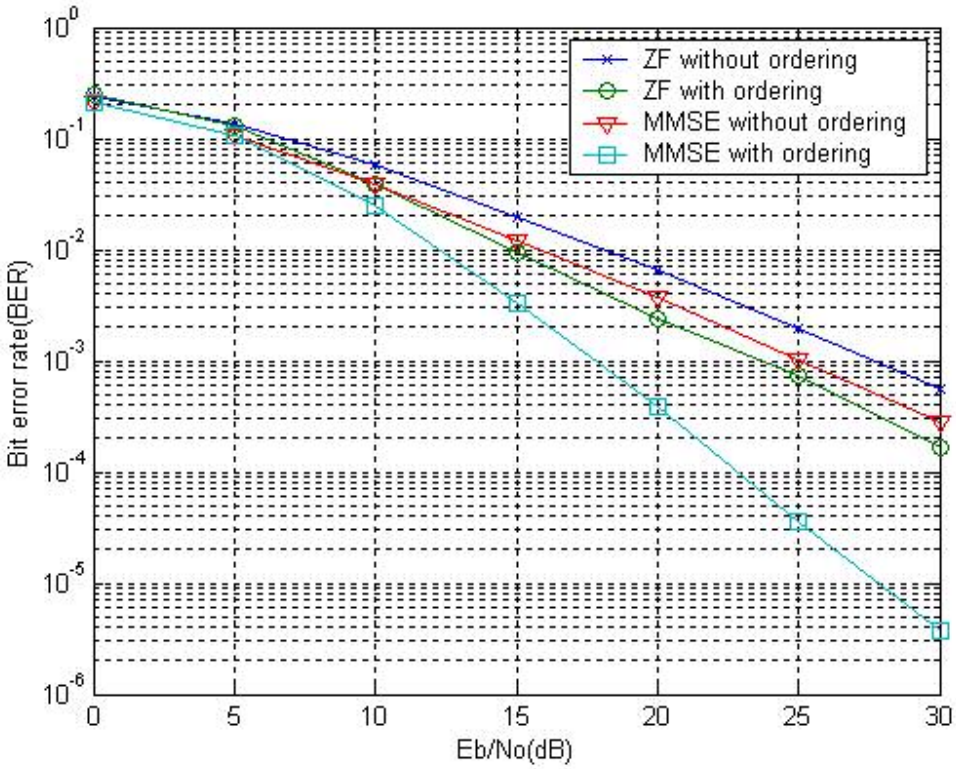

Figure 3.3 Performance of SIC V-BLAST, ZF v.s. MMSE, with and without ordering, 4Tx-4Rx, QPSK modulation, and perfect channel estimation.

3.2.2 Parallel Interference Cancellation

The PIC-based V-BLAST detector does not obtain the gain with applying the ordering of the layers. In the first stage, all layers with Eq. (3.5) are detected simultaneously.

$$\tilde{a} = G r, \tag{3.5}$$

where G is the pseudo-inverse matrix of the channel matrix with size $n_T \times n_R$, r is the received symbol vector and $\tilde{a}$ is a vector form of all detected layers. Eq. (3.6) describes the cancellation process, which subtracts the interference of the other $(n_T - 1)$ layers. The received signal after first step interference cancellation is formulated by

$$r_k = r - \sum_{j \neq k} \tilde{a}_j (H)_j \,, \tag{3.6}$$

where r_k is the received symbol vector applied with the interference cancellation of all but the k^{th} layer, $(H)_j$ is the j^{th} column vector of channel matrix and $\tilde{a}_j$ is the computed j^{th} layer symbol, that is the j^{th} element of the estimated symbol vector. In the second stage, the new nulling matrix is recalculated with the channel matrix nulling out the all but the k^{th} layer. Therefore, the nulling matrix becomes a row vector with size $(1 \times n_R)$ as Eq. (3.7).

$$G_k = C H_k^{+} \,. \tag{3.7}$$

By multiplying r_k from Eq. (3.6) with G_k from Eq. (3.7), the PIC-based V-BLAST detector recovers the all components of the transmitted symbol vector a. The performance of PIC based V-BLAST is shown in Figure 3.4 with the ZF and the MMSE nulling scheme. The MMSE nulling achieves about 2 dB gain more compared to the ZF, even if both schemes do not take the benefit of ordering of layers.

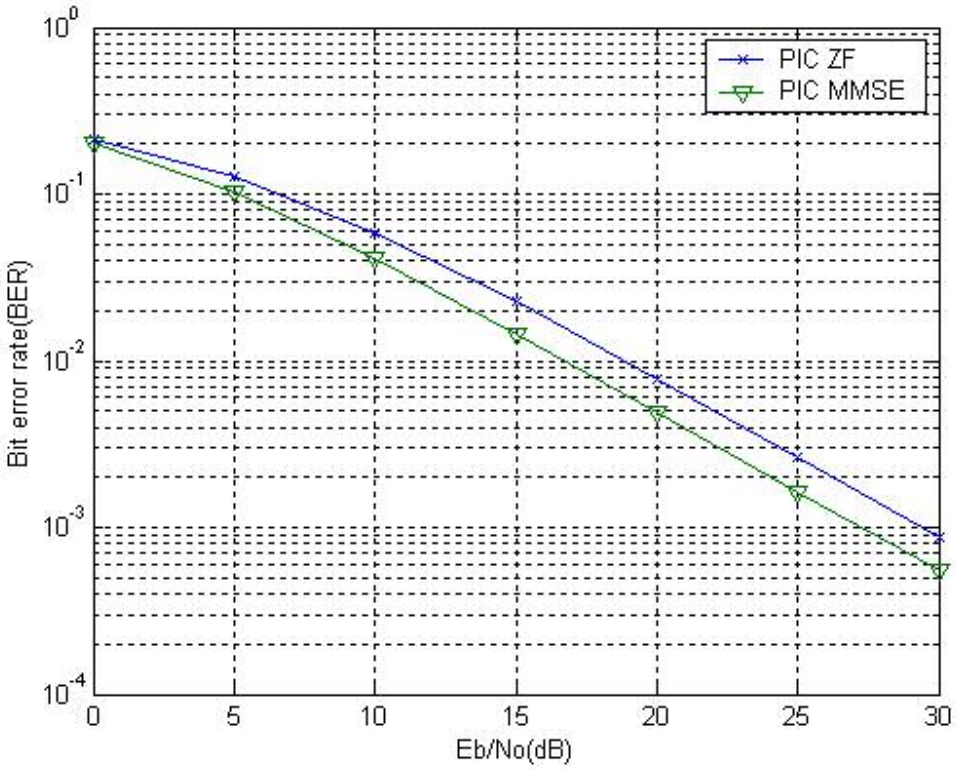

Figure 3.4 Performance of PIC V-BLAST, ZF v.s. MMSE, 4Tx-4Rx, QPSK modulation, and perfect channel estimation.

However, we can also get the benefit of ordered layer by substituting the first stage detection expressed in Eq (3.5) with SIC algorithm. Figure 3.5 illustrates this result in the case of a ZF nulling scheme. The PIC scheme employing SIC algorithm at first stage can take advantage of the ordering technique and also get the benefits of performance gain obtained by a multistage detector. Figure 3.5 shows that the combined scheme is improved by 1.5 dB compared to the SIC ordering scheme. We observe that the PIC detector achieves similar performance to SIC with no ordering. In the range of low SNR, the performance of the PIC detector is slightly better than SIC based on the non-

ordered scheme, whereas the performance of PIC detector degrades by 1 dB compared to that of SIC detector at high SNR range.

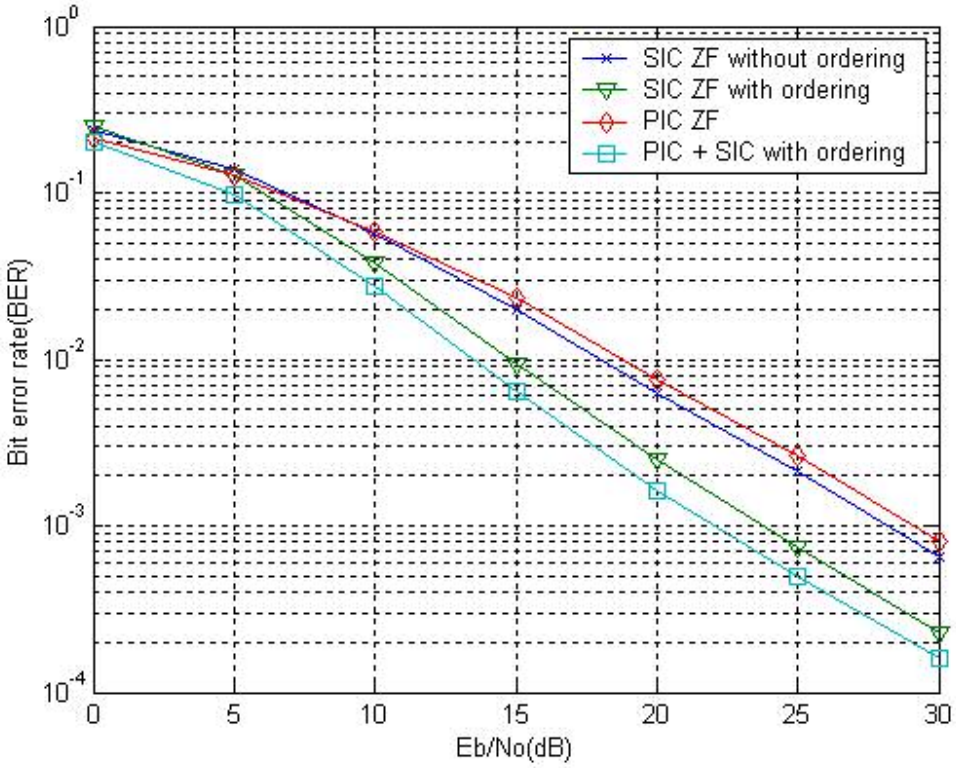

Figure 3.5 Comparison between SIC and PIC V-BLAST, ZF nulling, with and without ordering, 4Tx-4Rx, QPSK modulation, and perfect channel estimation.

3.3 Effect of Error Propagation

The performance of V-BLAST is constrained by the accuracy of the symbols recovered in the previous layer or in the previous stage corresponding to SIC and PIC respectively. These decision errors that are fed back are called error propagation. The error propagation problem contributes to the degraded bandwidth efficiency.

In the case of SIC-based V-BLAST, the received signal after cancellation of (k-1) layers is

formulated by

$$r_{i+k} = H_k\, a_k(i) + \sum_{j=1}^{k-1} H_j\,(a_j(i) - \tilde{a}_j(i)) + \sum_{j=k+1}^{n_T} H_j a_j(i) + v(i)\ , \tag{3.8}$$

where the first term represents the desired layer , the second term represents the inference from $(k-1)$ cancelled layers, the third term represents $(n_T - k)$ uncancelled layers and final term is for AWGN. Under the assumption of ideal cancellation, the second term is equal to zero because $a_j(i) = \tilde{a}_j(i)$ so that the error propagation does not occur.

The effect of error propagation on SIC-based V-BLAST is illustrated in Figure 3.6. In this result, the performance of individual layers of 4Tx-4Rx systems is compared with and without error propagation. The ZF nulling algorithm is applied for this comparison. For simulation of the case without error propagation, the receiver is assumed to have exact knowledge of all symbol layers that are cancelled at each iteration. Here, we observe that the slope increases as the nulling scheme proceeds from layer to layer with perfect interference cancellation since the diversity advantage is utilized. On the contrary, the case of non-perfectly interference cancellation suffers from error propagation so that the potential enhancement in diversity is not achieved and the BER slope of the successive layers does not become steep compared with the ideal cancellation case.

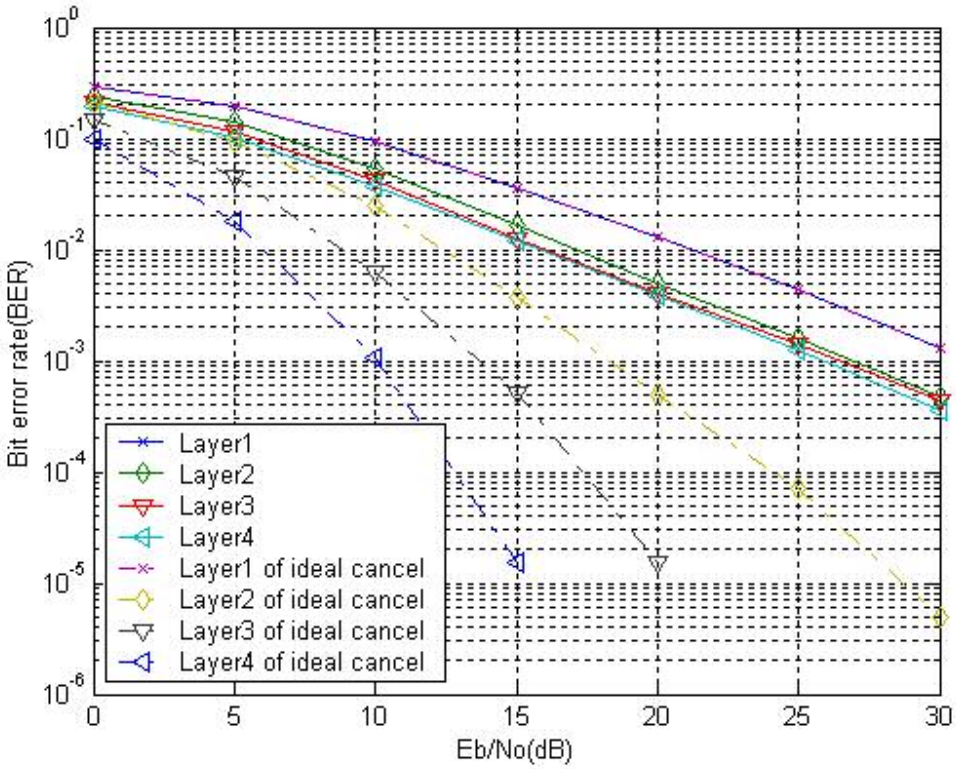

Figure 3.6 Effect of error propagation of SIC V-BLAST system, 4Tx-4Rx, QPSK modulation, ZF nulling, without ordering, and perfect channel estimation.

In the case of PIC-based V-BLAST, the received signal after first stage cancellation is formulated by

$$r_k(i+1) = H_k\, a_k(i) + \sum_{j \neq k} H_j\,(a_j(i) - \tilde{a}_j(i)) + v(i) \quad , k \in \{1, \cdots, n_T\}, \tag{3.9}$$

where the first term represents desired layers , the second term represents the inference from $(n_T - 1)$ cancelled layers and the final term is for AWGN. Under the assumption of ideal cancellation, the second term is equal to zero because $a_j(i) = \tilde{a}_j(i)$. The error propagation is illustrated in Figure 3.7. These observations lead us to conclude that the accuracy of previously

recovered layers has a significant impact on the overall performance.

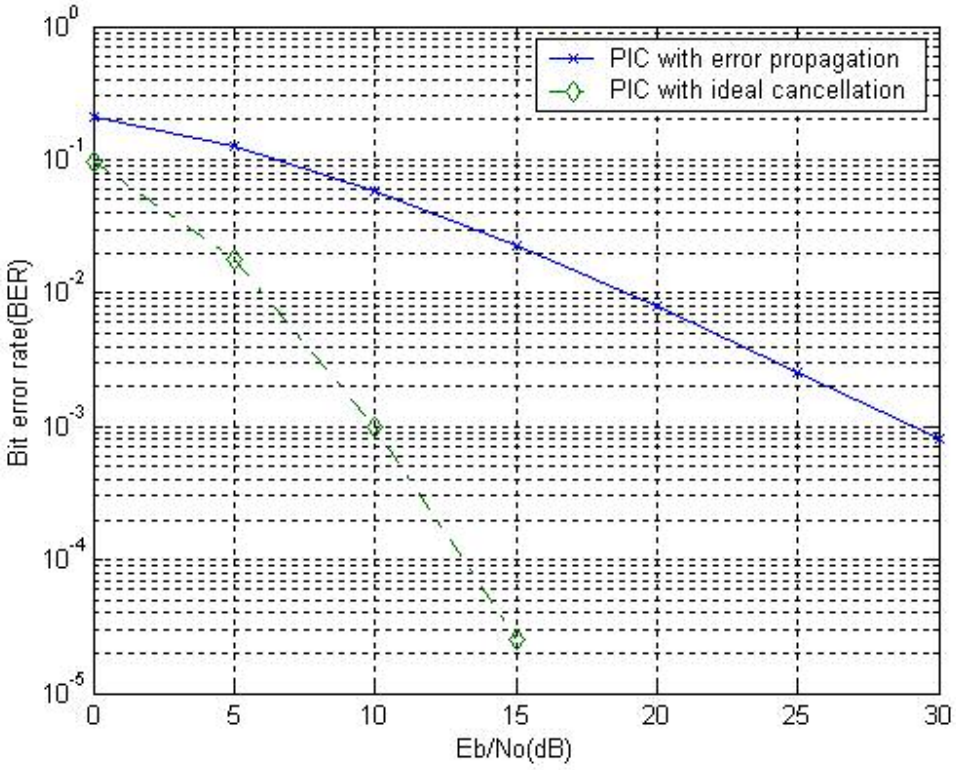

Figure 3.7 Effect of error propagation of PIC V-BLAST system, 4Tx-4Rx, QPSK modulation, ZF nulling, and perfect channel estimation.

3.4 Chapter Summary

In this chapter, we described V-BLAST structures and investigated the improvement obtained by an MMSE solution compared to a ZF solution and the performance gain of the ordered scheme over the non-ordered scheme. Additionally, the successive interference cancellation and parallel interference cancellation algorithms were reviewed. A method combining PIC and SIC algorithms was evaluated. Furthermore, the error propagation for both successive interference cancellation and

parallel interference cancellation V-BLAST detectors was presented. As in Chapter Two, the results presented here mirror those already published in the literature. However, in the next chapter where we investigate the performance of V-BLAST in a multi-user environment, we will explore performance trade offs that have not previously been investigated in the literature.

Chapter 4

Multi-user Detection with V-BLAST on MIMO

High data rate demanded in wireless communication motivates multiple antenna systems combined with multiuser detection schemes. The performance of multiuser detection along a MIMO downlink system is presented in [22]. A system to enhance signal-to-noise plus noise ratio for MIMO CDMA communications in the downlink for frequency-selective fading environments is considered in [23]. The performance of the V-BLAST algorithm combined with multi-user detection in downlink system is evaluated in [24]. There are various receiver structures for MIMO multiuser systems such as V-BLAST and Turbo-BLAST combined with multiuser detection schemes. In this thesis, we focus on the V-BLAST system combined with mutiuser detection schemes without channel coding, especially for the uplink. The structure of a downlink system is much simpler since the MIMO channel is shared to all users. In this downlink system, we can recover the all user's signals by applying various multiuser diction schemes only after equalizing the shared channel. However, for the reverse link, the structure of receivers is more complicated since the channels vary between users. This chapter is organized as follows. In Section 4.1, the system model is introduced. Section 4.2 provides linear and non-linear receiver structures and formulates a detecting algorithm. Comparative simulation results are presented and analyzed in Section 4.3. Finally, Section 4.4 summarizes this work.

4.1 System Model

The received baseband signal from K users is formulated by

$$r(t) = \sum_{k=1}^{K} H^k s_k(t-\tau_k) + n(t) \tag{4.1}$$

$$s_k(t-\tau_k) = \sqrt{P_k}\, a_k(t-\tau_k)\, c_k(t-\tau_k) e^{j\theta_k}, \tag{4.2}$$

where the received signal is a vector form like $r(t) = [r^1(t)\ r^2(t) \cdots r^{n_R}(t)]^T$. The superscripts of elements of the received signal vector represent the n_R th receive antennas. H^k represents channel matrix for MIMO channel fading affecting the k^{th} user with size $n_T \times n_R$ whose element $h_{i,j}^k$ is the complex fading coefficient for the path from transmit antenna j to receive antenna i. These fading coefficients are modeled as an independent complex Gaussian random variable with zero mean and variance 0.5 per dimension. a_k represents the vector of transmitted symbols with dimension $n_T \times 1$ like $a_k(t) = [b_k^1(t)\ b_k^2(t) \cdots b_k^{n_T}(t)]^T$ whose components are the data symbols. That is, a_k is made to demultiplex input data stream b_k. This demultiplexing is the encoding scheme for the V-BLAST at the transmitter. τ_k is the time delay that models the asynchronous nature of uplink system. τ_k needs not to be considered in down link system. θ_k is the received phase of the k[th] user relative to an arbitrary reference phase, P_k is the k^{th} user's received signal power and $c_k(t)$ represents spreading sequences. Figure 4.1 illustrates the system model.

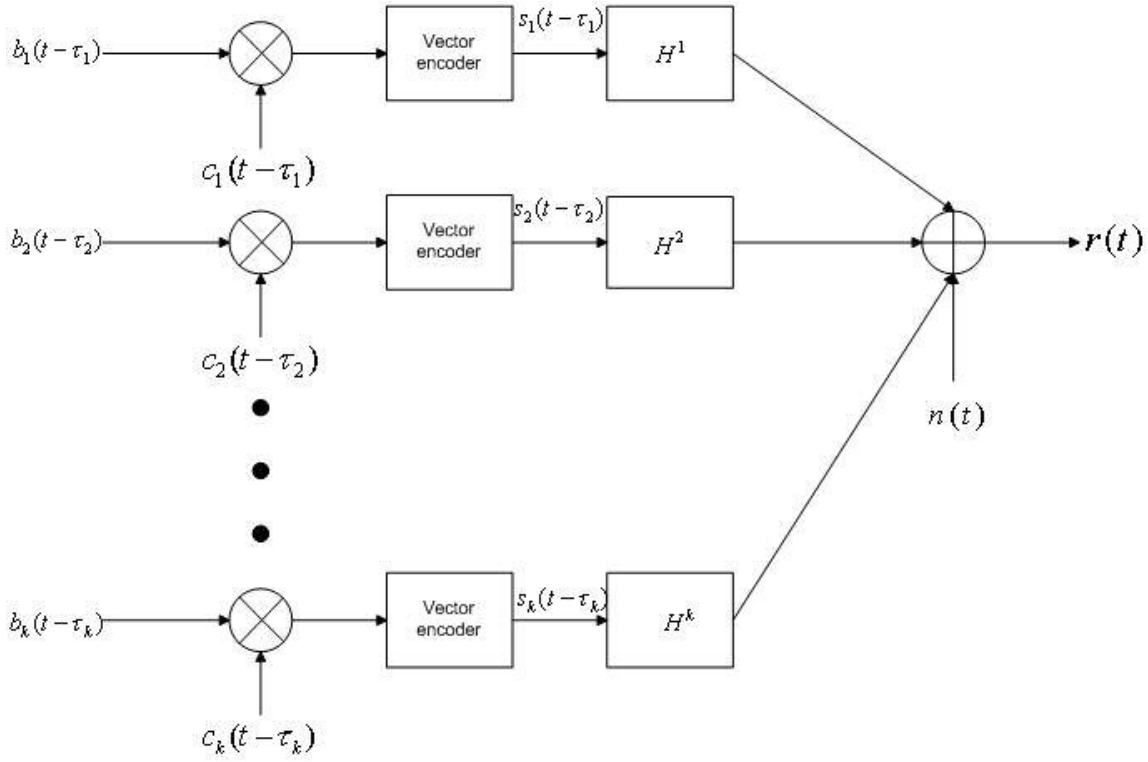

Figure 4.1 Multi-user V-BLAST System Model on MIMO channel.

4.2 Multi-user Receivers

4.2.1 Conventional Receiver

The receiver structure is made up of a matched filter bank at each antenna point followed by the V-BLAST decoding block. The outputs of the matched filter banks are rearranged in the form of vector for each corresponding user. The matched filter output y^{i} at the i^{th} antenna, which is despread by each user's spreading sequence, is formulated by

$$\mathrm{y}^{\mathrm{i}} = RW\mathrm{X}^{\mathrm{i}} + \mathrm{n} \quad \mathrm{i}=1,2\cdots n_R, \tag{4.3}$$

where R is a correlation matrix size $KN_f \times KN_f$.

$$R = \begin{pmatrix} \mathrm{R}(0) & \mathrm{R}(-1) & 0 & \cdots & 0 \\ \mathrm{R}(1) & \mathrm{R}(0) & \mathrm{R}(-1) & & \vdots \\ 0 & \mathrm{R}(1) & \mathrm{R}(0) & \ddots & \\ \vdots & \vdots & \vdots & \ddots & \mathrm{R}(-1) \\ 0 & \cdots & 0 & \mathrm{R}(1) & \mathrm{R}(0) \end{pmatrix} \tag{4.4}$$

The element $\mathrm{R}(i)$ with size $K \times K$ is defined by

$$\rho_{l,m}(i) = \int_{-\infty}^{\infty} c_l(t-\tau_l)\, c_m(t+iT-\tau_m) dt\,, \tag{4.5}$$

where T is the symbol duration. W represents the $KN_f \times KN_f$ diagonal matrix of the square root of user received energies. N_f is the number of consecutive symbols and K is the total number of users loaded in the system. X^{i} is the KN_f length vector form of all users' data symbols transmitted over the MIMO channel described in Eq (4.6). Each element is expressed as in Eq (4.7)

$$\mathrm{X}^{\mathrm{i}} = [x_1^i(1)\ x_2^i(1) \cdots x_k^i(1)\ x_1^i(2)\ x_2^i(2) \cdots x_k^i\ x_1^i(N_f)\ x_2^i(N_f) \cdots x_k^i(N_f)]^T\,, \tag{4.6}$$

$$x_k^i(l) = \sum_{j=1}^{n_T} h_{i,j}^k b_j(l)\ ,\ l = 1, 2, \cdots, N_f\ . \tag{4.7}$$

The statistics are manipulated by the V-BLAST decoding algorithm after the matched filter operation. Here, the operator $\mathbb{Q}_{G^k}$ is defined for convenience as the V-BLAST decoding processing with the nulling matrix G^k, which represents the pseudo-inverse channel matrix of k^{th} user. The pseudo-inverse channel matrix is represents by

$$G^k = (H^{k+} H^k)^{-1} H^{k+}\ , \tag{4.8}$$

$$G^k = (H^{k+}H^k + \frac{\sigma_n^2}{\sigma_d^2})^{-1} H^{k+}. \quad (4.9)$$

Eq. (4.8) is a pseudo-inverse channel matrix for the ZF nulling criterion and Eq. (4.9) is for the MMSE nulling criterion, which are described in Chapter 2. This operation cancels the multiple antenna or spatial interference caused by the V-BLAST decoding algorithm in the manner of parallel interference cancellation or serial interference cancellation. Therefore, the recovered symbols are represented by

$$\tilde{b}_k = \mathbb{Q}_{G^k}([y_k^1 \; y_k^2 \cdots y_k^{n_R}]^T) \;\; k = 1, 2 \cdots, K. \quad (4.8)$$

The desired signal within a conventional receiver cannot avoid the interference from other user's signals especially in an asynchronous system since the correlation matrix contributes the decision of transmitted symbols even in V-BLAST as discussed in Chapter 3. In the next sections, we will introduce linear interference cancellation and non-linear interference cancellation schemes.

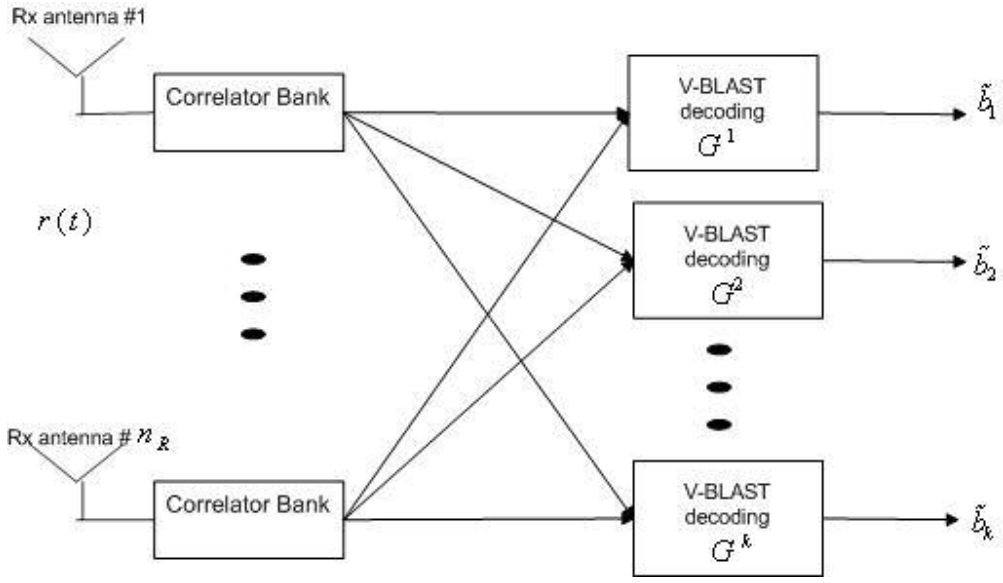

Figure 4.2 Structure of conventional receiver for V-BLAST multiuser system.

4.2.2 Decorrelating Receiver

The decorrelating receiver is a linear detector that performs interference cancellation by linear transformation for finding the decision metric.

As a first step, we need to eliminate the interference from undesired signals by

$$\mathrm{z}^{\mathrm{i}} = \mathrm{T}\ \mathrm{y}^{\mathrm{i}} \quad \mathrm{i}=1,2\cdots n_R \tag{4.9}$$

$$\mathrm{z}^{\mathrm{i}} = [z_1^i(1)\ z_2^i(1)\cdots z_k^i(1)\ z_1^i(2)\ z_2^i(2)\cdots z_k^i\ z_1^i(N_f)\ z_2^i(N_f)\cdots z_k^i(N_f)]^T \tag{4.10}$$

The linear transformation, $\mathrm{T}= R^{-1}$, is obtained from the maximization of the likelihood function or equivalently the minimization of $\Lambda(\Theta) = (\mathrm{y} - R\Theta)^T R^{-1}(\mathrm{y} - R\Theta)$ where y represents the output of matched filter and Θ is estimated signal.

More explicitly

$$\mathrm{z}^{\mathrm{i}} = R^{-1}\ \mathrm{y}^{\mathrm{i}} \quad \mathrm{i}=1,2\cdots n_R \tag{4.11}$$

$$= W\mathrm{X}^{\mathrm{i}} + R^{-1}\mathrm{n} \quad \mathrm{i}=1,2\cdots n_R . \tag{4.12}$$

At the second step, after rearranging the decorrelated singals, the V-BLAST decoding algorithm is applied to the signal z^{i} where the spatial interference of undesired signals is reduced and the symbols are decided as follows:

$$\tilde{b}_k = \mathbb{Q}_{G^k}([z_k^1\ z_k^2\cdots z_k^{\mathrm{n_R}}]^T)\ \ k = 1,2\cdots,K . \tag{4.13}$$

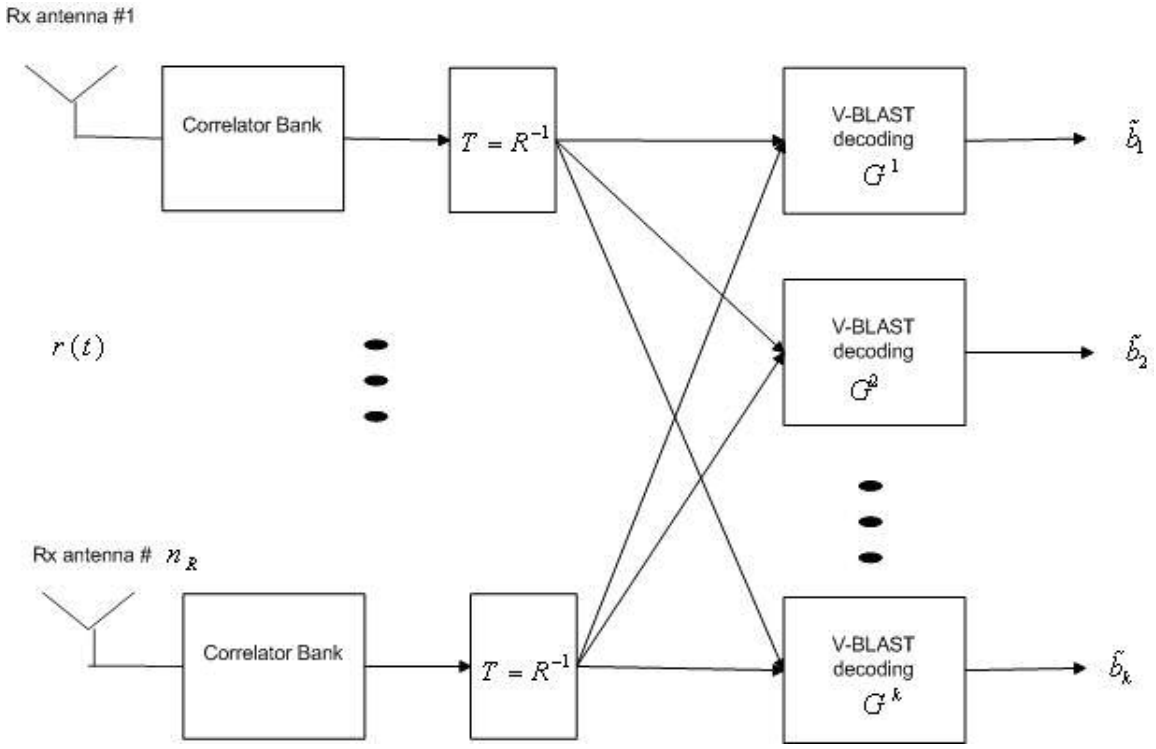

Figure 4.3 Structure of decorrelator for V-BLAST multiuser system.

4.2.3 MMSE Receiver

Another type of linear detector can be obtained if the linear transformation is sought which minimizes the mean squared error between the transmitted symbols and the outputs of the transformation $E\{(\Theta - T\mathrm{y})^T(\Theta - T\mathrm{y})\}$, that is, the MMSE criterion. Therefore, the linear transformation of decorrelating receiver used in previous section is replaced by $\mathrm{T} = (R + N_0 / 2W^2)^{-1}$ for MMSE multiuser detection.

$$\mathrm{z}^{\mathrm{i}} = (R + N_0 / 2W^2)^{-1}\ \mathrm{y}^{\mathrm{i}} \quad \mathrm{i}=1,2\cdots n_R \tag{4.14}$$

As a spatial interference cancellation step, the V-BLAST decoding block is the same as for the decorrelator by

$$\tilde{b}_k = \mathbb{Q}_{G^k}([z_k^1 \; z_k^2 \cdots z_k^{n_R}]^T) \;\; k = 1, 2 \cdots, K \tag{4.15}$$

4.2.4 Multistage Parallel Interference Cancellation

A muultistage interference cancellation technique for the SISO channel is proposed in [11] and developed in [9]. We apply this technique to a MIMO channel system with the V-BLAST algorithm. The simple two-stage detector is illustrated in Figure 4.4. In this detector, the matched filter bank is used at the first stage even though any type of detector such as a decorrelator or a MMSE receiver can be utilized. The performance of MPIC highly depends on the accuracy of the first stage detector since this technique reduces the multiple access interference by subtracting the interferers detected at previous stage from desired signals. Therefore, the number of stages becomes a significant factor for improving BER performance, whereas the structure of the receiver gets more complicated as the number of receiver stages becomes large. Also, powerful channel coding such as Turbo-BLAST contributes to improved performance of MPIC and reduces the number of stages. However, we will only consider characteristics of a MPIC receiver without channel coding. As shown in Figure 4.4, each element of received signal vector goes through the matched filter banks. Each matched filter bank at each receive antenna provides the output of K users estimated signal. This output is arranged in a vector form whose elements correspond to k^{th} user's signal. As a next step, the V-BLAST algorithm is applied with the pseudo-inverse channel matrix $G^k \;\; k = 1, 2 \cdots, K$ to reduce the spatial interference. This output is the estimated signal at the first stage. In order to mitigate the multiple access interference, we spread the estimated signals at the first stage with each user's spreading sequence. Then, these regenerated signals experience the MIMO channel matrix, which should be estimated via a pilot channel estimation technique. We expect that multiple access

interference cancellation at the next stage relies heavily on the accuracy of recovered symbols from the first stage and also the accuracy of the channel estimation. Subtracting the regenerated signals from the received signals $r(t)$ results in the multiple access interference cancellation. Iteratively, we can recover the transmitted signal of all users at subsequent stages by using updated received signals.

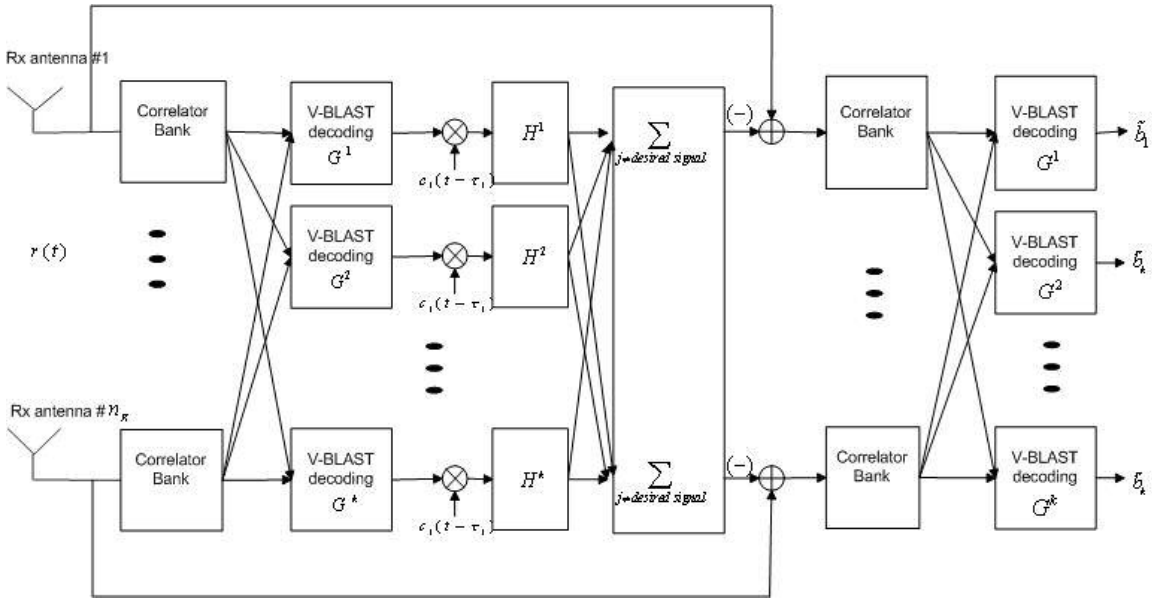

Figure 4.4 Structure of two-stage detector for V-BLAST multiuser system.

Mathematically, we can describe the decision metric for s-stage parallel interference cancellation scheme as follows:

$$\tilde{b}_k = \mathbb{Q}_{G^k}\left([y_k^{1,(s)}\ \ y_k^{2,(s)}\cdots y_k^{n_R,(s)}]^T\right)\ \ k=1,2\cdots,K\,, \tag{4.16}$$

where

$$y_k^{i,(s)} = \frac{1}{T}\int r_k^{i,(s)}(t)\ c_k(t-\hat{\tau}_k)\ dt,\ i=1,2\cdots,n_R,\ k=1,2\cdots,K \tag{4.17}$$

$$r_k^{i,(s)}(t) = r(t)^i - \sum_{j\neq k} y_j^{(s-1)}\ c_j(t-\hat{\tau}_j),\ i=1,2\cdots,n_R, k=1,2\cdots,K. \tag{4.18}$$

The superscript i represents the receive antenna number, k is the user number, $r_k^{i,(s)}(t)$ represents the s-stage signal of the k^{th} user at antenna i after cancellation, c_k represents the spreading sequence of the k^{th} user, and $\tilde{\tau}_k$ represents the estimated time delay of the k^{th} user. The operator $\mathbb{Q}_{G^k}$ represents the V-BLAST decoding processing.

A bias reduction technique for multistage interference cancellation is verified in [6]. The bias increases linearly with system loading such that the bias influences the decision statistics in the first stage of multiple access interference cancellation. The effect of bias is mitigated for subsequent stages. To reduce the effect of bias, a partial-cancellation factor $C^{(s)}$ is employed. This factor varies at every stage in the range [0,1]. The partial-cancellation factor $C^{(2)}$ of 0.5 at second stage gives good performance improvement [12]. The mathematical form of cancellation with the partial-cancellation factor is formulated by

$$r_k^{i,(s)}(t) = r(t)^i - C^{(s)}\sum_{j\neq k} y_j^{(s-1)}\ c_j(t-\hat{\tau}_j),\ i=1,2\cdots,n_R, k=1,2\cdots,K. \tag{4.19}$$

4.3 Simulation Results and Analysis

In this section, we compare the performance of four types of multiuser receivers combined with V-BLAST under asynchronous MIMO channels. Perfect power control, perfect channel estimation and time delay estimation are assumed. The Rayleigh flat fading channel is considered. We define one

frame as one packet of 20 symbols. The channel coefficients are modeled with an independent zero mean complex Gaussian random variable with variance 0.5 per dimension. The channel coefficients are constant during one frame transmission, that is, they are changed at every 20 symbols. Gold sequences with 31 processing gain are utilized. Each chip of the spreading sequences is sampled at 5 samples/chip. Timing delays are generated randomly to realize an asynchronous model. The ZF nulling V-BLAST algorithm based on successive spatial interference cancellation is employed.

The capacity curve Figure 4.5 with $E_b / N_o = 20dB$ depicts the performance of three-stage PIC with the various partial-cancellation factors at second stage. For the lightly loaded system, partial-cancellation factors of 0.7 and 0.9 give good reduction of the multiple access interference at the second stage. However, partial-cancellation factors of 0.7 and 0.5 mitigate the effect of bias relatively well for a highly loaded system. Considering all cases, the partial-cancellation factor 0.7 can be considered as the best choice at flat fading MIMO channel.

The capacity curves for $E_b / N_o = 20dB$ and processing gain $N = 31$ are shown in Figure 4.6. For this result, we observe that the performance of the decorrelator, MMSE detector and two-stage PIC combined with decorrelator at first stage are equivalent. Additionally, they exhibit enormous performance improvement compared to the conventional receiver. However, the performance of the three-stage PIC receiver, that is a non-linear interference cancellation receiver, gradually degrades as the number of active users increase even though it outperforms the conventional receiver. Figure 4.7 illustrates results for a system with 10 users, showing how the number of stages affects the performance improvement for multistage PIC. The Figure 4.7 shows how the number of stages affects the performance improvement of multistage PIC. We observe that the performance of MPIC is improved as the number of stages increases. However, the MPIC performance does not equal the

performance of linear detectors such as the decorrelator and the MMSE receiver since the multiple antenna interference prevents the MPIC receivers from canceling out the multiple access interference appropriately. We recognize that the multiple antenna interference affects the performance of the non-linear multiple access interference cancellation receiver. Therefore, the MPIC receivers are not suitable without a channel coding scheme for MIMO channels.

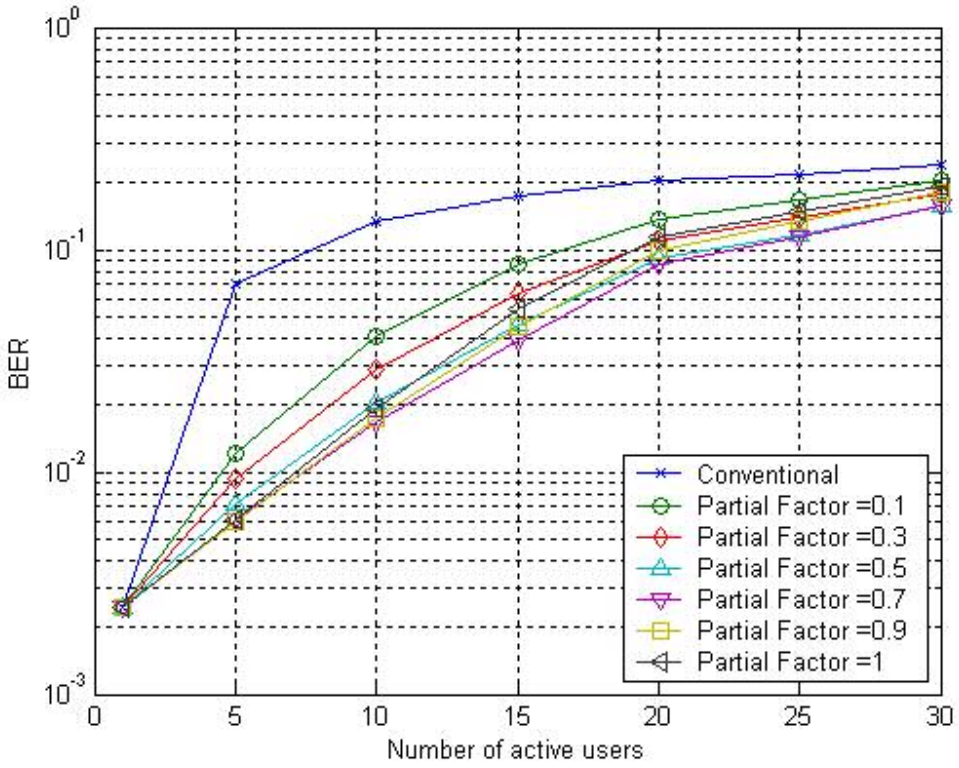

Figure 4.5 BER versus number of active users as influenced by partial-cancellation factor for MPIC in Flat Fading MIMO channels. QPSK modulation, perfect channel estimation, ZF nulling, $E_b / N_o = 20dB$, Gold sequences with a processing gain of 31.

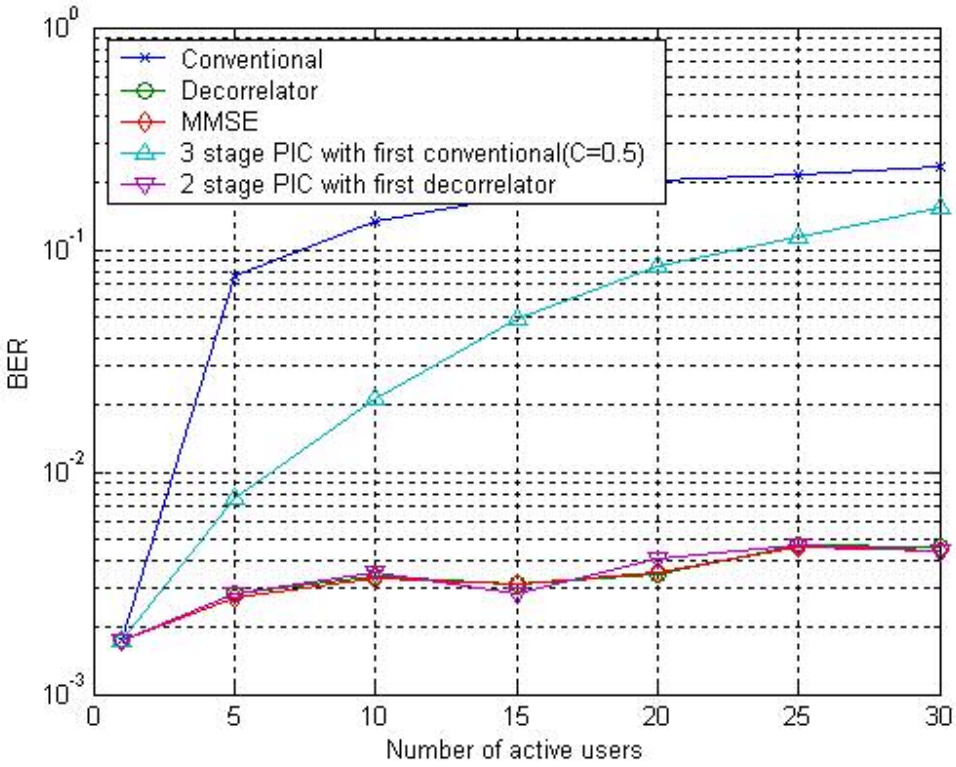

Figure 4.6 BER versus number of active users with perfect channel estimation in Flat Fading MIMO channels. QPSK modulation, ZF nulling, $E_b / N_o = 20dB$ and Gold sequences with a processing gain of 31

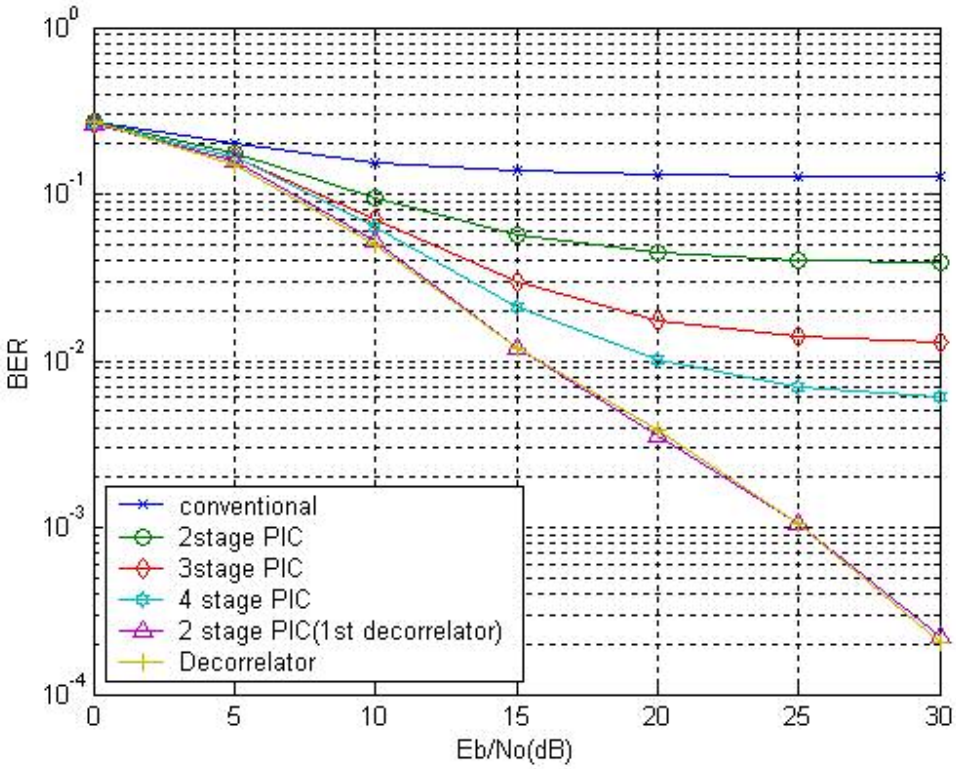

Figure 4.7 BER versus Eb/No with perfect channel estimation under Flat fading MIMO channels. QPSK modulation, ZF nulling, Gold sequences with a processing gain of 31 and 10 active users.

4.4 Chapter Summary

In this chapter, we investigated the receiver structure of multiuser detectors combined with V-BLAST to MIMO. The performance of MPIC receivers with various partial-cancellation factors was verified. All receivers such as the decorrelator, MMSE and MPIC achieve the tremendous performance improvement compared to the conventional receiver that does not eliminate multiple access interference. However, the MPIC receiver, which is one of the nonlinear detectors, over the MIMO channels is not robust to interference from multiple antennas that obstructs cancellation at

each stage, whereas linear detectors are not as severely affected by multiple antenna interference.

Chapter 5

Effect of Parameter Estimation Error

5.1 Channel Estimation

One of crucial parts of the communication system is the block that estimates the channel. In the previous chapters, we assumed that the receiver has the perfect knowledge of the channel. Algorithms for channel estimation can be either block-based or adaptive. For example, a training sequence adaptive algorithm such as recursive least squares (RLS) or least mean squares (LMS) is based on detected symbols [25]. Since the real channel is varying in time, this requires a technique that continuously estimates the channel. However, the assumption that the channel is constant during the time of one data block, the so-called quasi-static channel, makes it possible to estimate the channel block wise. Therefore, we employ a block based MMSE estimate as a channel estimation algorithm. As a SISO channel model, a complex one-tap filter $h = \alpha e^{j\theta}$ is used, where α is the magnitude of channel and θ is the phase delay of channel. The channel filter is calculated by choosing h that minimizes the error $J(h)$.

$$J(h) = E\{|r(n) - ht(n)|^2\}, \tag{5.1}$$

where $J(h)$ represents the received signal and $J(h)$ represents the training or pilot sequence. According to the MMSE-criterion, the signal tap channel is estimated by [2]

$$\tilde{h} = \sum_{tt}^{-1} \sum_{tr}, \tag{5.2}$$

where

$$\sum_{tt} = E\{t(n)t^*(n)\}, \tag{5.3}$$

$$\sum_{tr} = E\{t(n)r^*(n)\}. \tag{5.4}$$

Eq. (5.3) and Eq.(5.4) represent the autocorrelation of the training sequence and the cross-correlation between the training sequence and the received symbol respectively. * denotes the complex conjugate.

The baseline block channel estimation algorithm can be extended to a MIMO system [26].

Let the system be represented by a baseband model with n_T transmitting antennas and n_R receiving antennas so that

$$\mathrm{y} = H\mathrm{x} + \nu. \tag{5.5}$$

The channel matrix H with size $n_R \times n_T$ represents the flat fading channel whose elements are complex numbers. y is the $n_R \times 1$ received signal vector, and x is the $n_T \times 1$ transmitted signal vector. It might be used as a training sequence vector for channel estimation. ν is a $n_R \times 1$ vector of complex additive white Gaussian noise with zero mean and unit variance. The block fading channels are estimated by the form of Eq (5.6)

$$\tilde{H} = \mathrm{Y}\,\mathrm{S}^{+}(\mathrm{SS}^{+})^{-1}, \tag{5.6}$$

where

$$\mathrm{Y} = [\mathrm{y}_1\ \mathrm{y}_2 \cdots \mathrm{y}_L], \tag{5.7}$$

$$\mathrm{S} = [\mathrm{s}_1\ \mathrm{s}_2 \cdots \mathrm{s}_L]. \tag{5.8}$$

The superscript + represents the conjugate transpose. Y is the matrix of received signal. S is the matrix form of the training symbol vector.

The training sequences are orthogonal across all transmitting antenna in order to minimize the mean

squared estimation error. It is necessary that the training length L be greater than or equal to the number of the transmit antennas n_T for the existence of the matrix inversion $(\mathrm{SS}^{+})^{-1}$.

The performance degradation due to the channel estimation error is illustrated from Figure 5.1 to Figure 5.4. Four symbols per antenna are used as a pilot for block-based channel estimation. Figure 5.1 and Figure 5.2 show BER curves for systems with 10 active users corresponding to SISO and MIMO channels respectively. Figure 5.2 and Figure 5.4 are capacity curves for $E_b / N_o = 20dB$ assuming SISO and MIMO channels respectively. The estimated channel error leads to an error floor of three-stage PIC receiver due to imperfect interference cancellation caused by the mismatched channel coefficients. The MPIC receiver has a feedback structure for interference cancellation; therefore the performance of MPIC relies heavily on the accuracy of channel estimation. However, the remaining receivers do not experience significant performance degradation. It is interesting to note that the performance of two-stage PIC with decorrelator at the first stage is worse than MMSE receiver or decorrelator only receiver at MIMO channel as shown in Figure 5.2 and Figure 5.4.

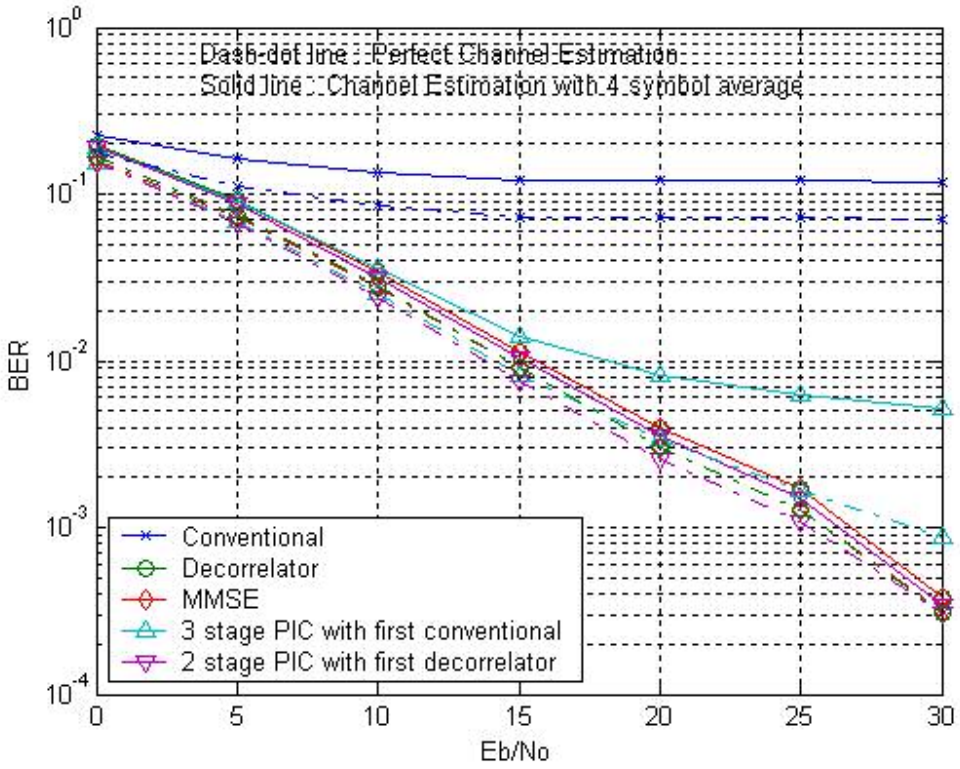

Figure 5.1 BER versus Eb/No illustrating the effect of channel estimation error for a SISO channel. QPSK modulation, channel estimation with 4 symbols average and 10 users are assumed.

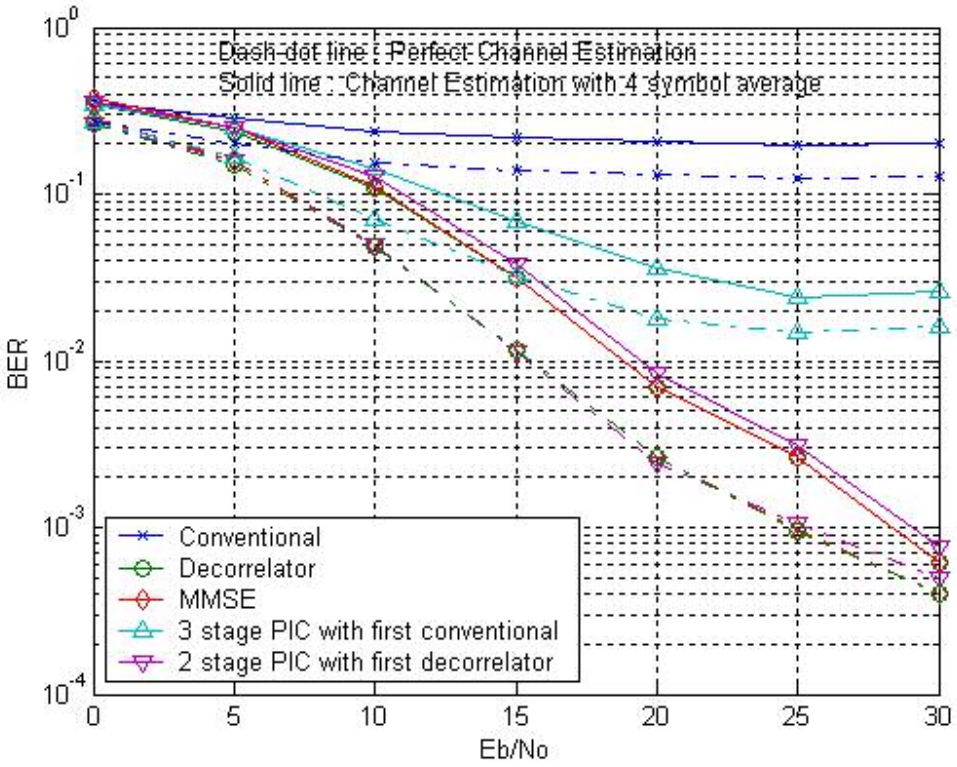

Figure 5.2 BER versus Eb/No, illustrating the effect of channel estimation error for a MIMO channel. QPSK modulation, ZF nulling, channel estimation with 4 symbols average and 10 users are assumed.

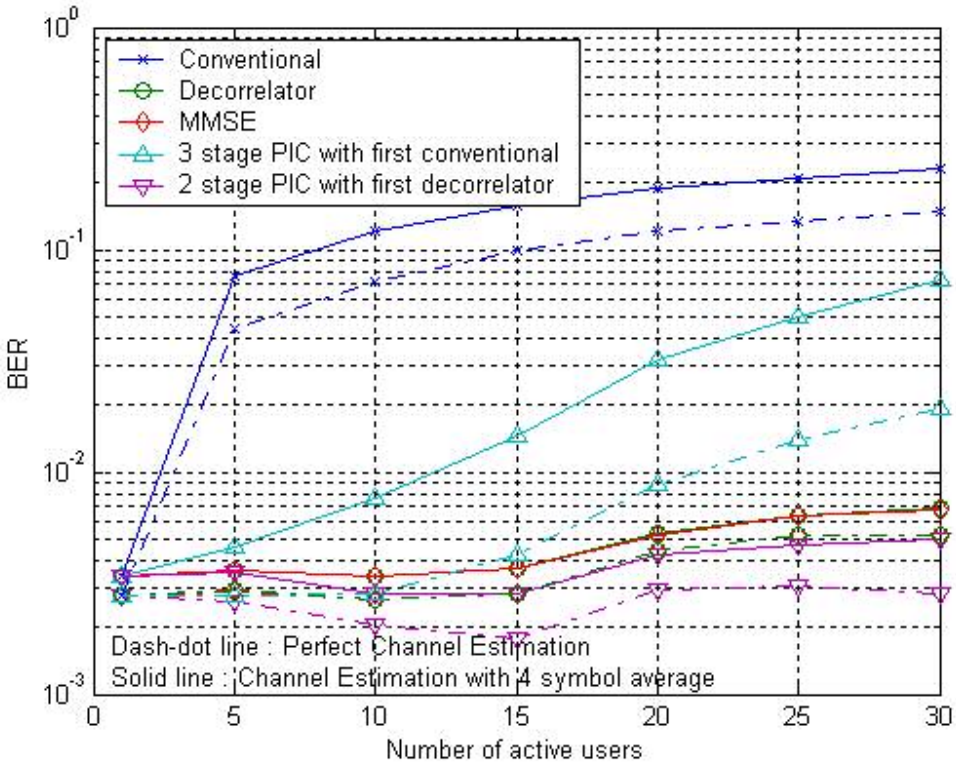

Figure 5.3 BER versus number of users, showing the effect of channel estimation error for a SISO channel. QPSK modulation, channel estimation with 4 symbols average and $E_b / N_o = 20dB$ are assumed.

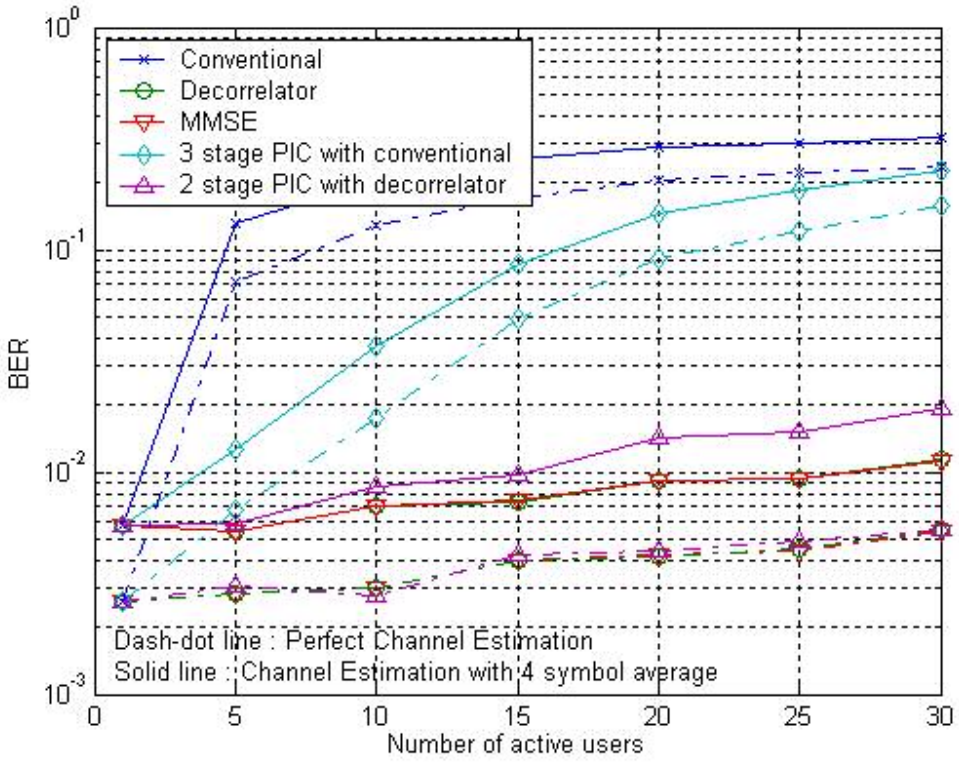

Figure 5.4 BER versus number of active users, showing the effect of channel estimation error for a MIMO channel. QPSK modulation, channel estimation with 4 symbols average and $E_b / N_o = 20dB$ are assumed.

5.2 Timing Delay Error

In the previous chapters, we assumed that the receiver was perfectly synchronized. However, in a real system, some timing delay error will occur. Thus we investigate the effect of timing delay error on the performance of multiuser detectors for both SISO and MIMO channels. The estimation error is simply assumed to be a Gaussian random variable with some standard deviation. In this simulation, we sampled each chip with ten samples. The effect of timing delay error for

$E_b / N_o = 8dB$ and 10 active users in an AWGN channel is shown in Figure 5.5. Figure 5.6 and Figure 5.7 illustrate the simulated result of effect of timing delay error for $E_b / N_o = 8dB$ and 10 active users in flat fading SISO and MIMO channels respectively. As shown in those figures, the performance degrades very rapidly as the error of timing delay estimation becomes large.

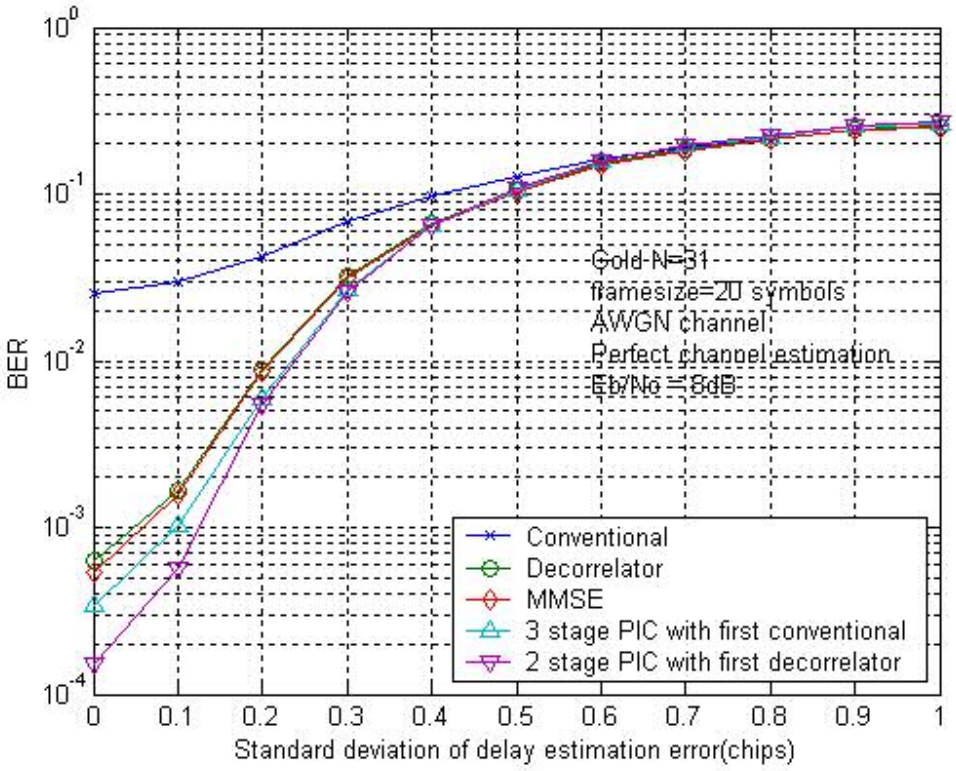

Figure 5.5 Effect of Timing Delay Estimation Error in an AWGN channel. QPSK modulation, perfect channel estimation, $E_b / N_o = 8dB$, a processing gain of 31 and 10 users are assumed.

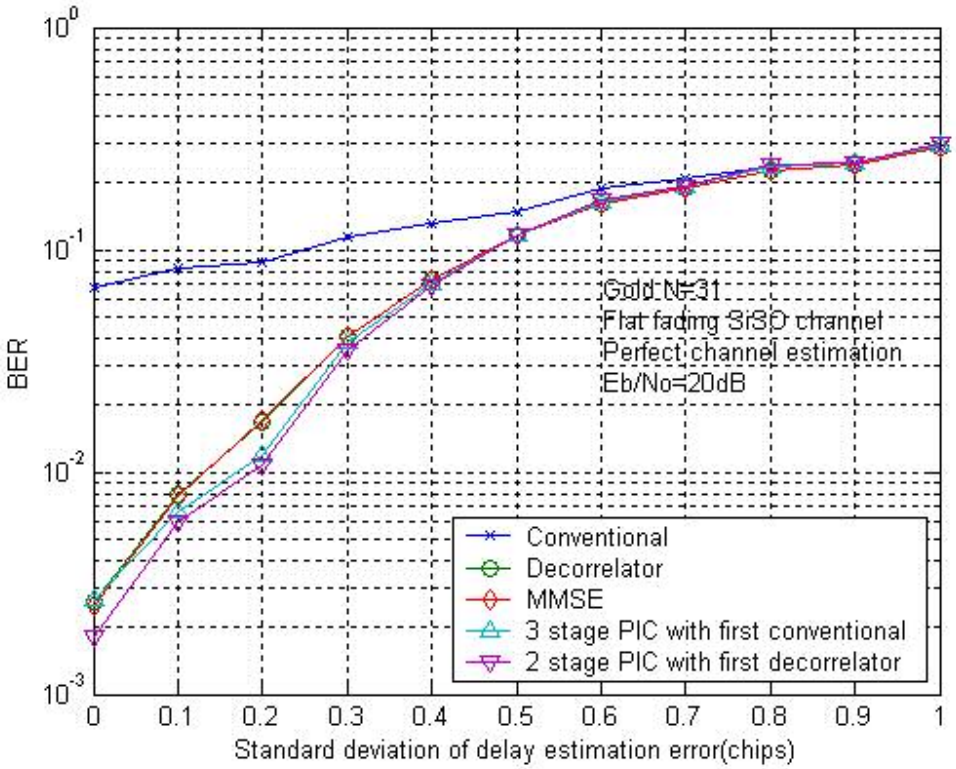

Figure 5.6 Effect of Timing Delay Estimation Error in a Flat fading SISO channel. QPSK modulation, perfect channel estimation, $E_b / N_o = 20dB$, a processing gain of 31 and 10 users are assumed.

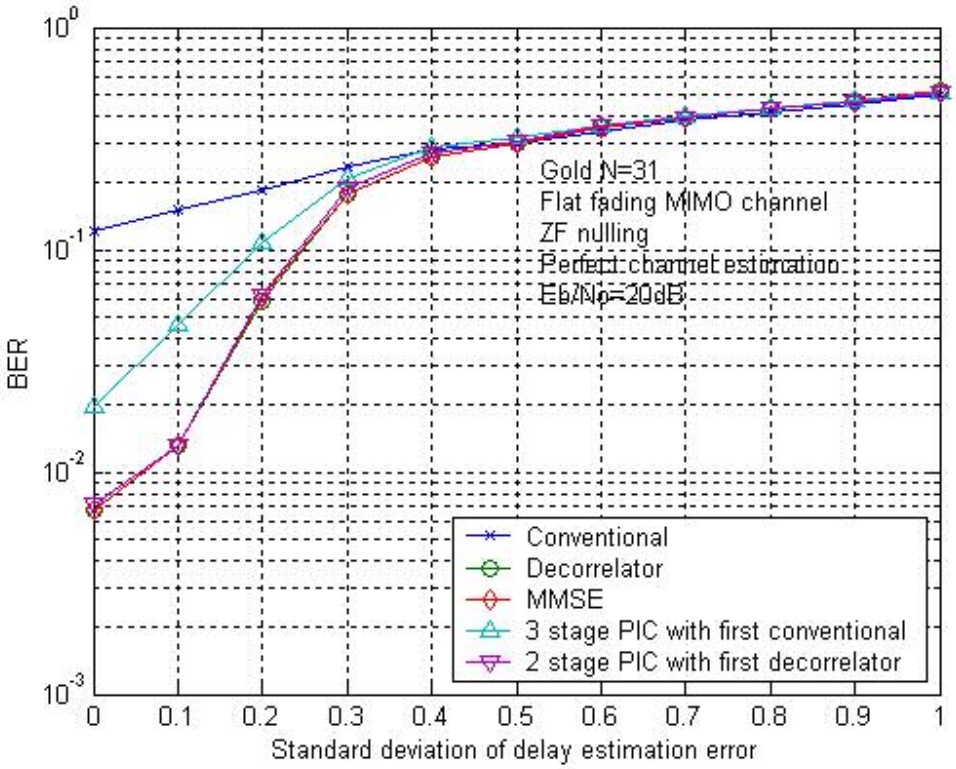

Figure 5.7 Effect of Timing Delay Estimation Error in a Flat fading MIMO channel. QPSK modulation, perfect channel estimation, $E_b / N_o = 20dB$, a processing gain of 31 and 10 users are assumed.

5.3 Chapter Summary

The effect of channel estimation error and timing delay estimation error was evaluated both in SISO and MIMO channels. The timing delay estimation is one of the critical factors of performance regardless of receiver structure, whereas the channel estimation error causes a greater impact on the performance of the non-linear multistage interference cancellation receiver.

Chapter 6

Conclusions

6.1 Summary of Results

In Chapter 2, the performance of the multi-user receivers at the base station was compared for an AWGN channel and a Rayleigh flat fading channel with the assumption of perfect knowledge of the channel and the exact timing delay estimation. The three-stage interference cancellation receiver, that is non-linear multiuser receiver, outperforms the linear multiuser receivers such as the decorrelator and the MMSE receiver for lightly loaded system. However, the non-linear receiver needs more stages to obtain equivalent performance to the linear receiver for a highly loaded system. All receivers result in performance improvement compared to conventional receiver. The bias reduction technique was evaluated for both an AWGN and a Rayleigh flat fading SISO channel.

In Chapter 3, the structure of V-BLAST was introduced. Parallel interference cancellation (PIC) and successive interference cancellation (SIC) based algorithms were reviewed and the performances of these were evaluated. The effect of error propagation was investigated for both the cases of PIC and SIC.

In Chapter 4, the receiver structures for multiuser V-BLAST system at a base station for a MIMO channel were illustrated. The performance of the receivers for a multiuer V-BLAST system was evaluated with assumption of perfect channel estimation and perfect timing delay estimation. The

receivers such as decorrelator, MMSE and MPIC receiver outperform the conventional receiver even in MIMO channels. However, the performance of MPIC receiver was highly degraded according to the system loading since the multiple antenna interference led to a strong impact on the performance degradation of a multistage interference cancellation receiver.

Finally, in Chapter 5 we investigated how the channel estimation and timing delay estimation error influences the performance of linear and non-linear multiuser receivers. The performance of MPIC receiver depends on the accuracy of channel estimation compared to that of the linear receivers and all of receivers are very rapidly degraded as the error of delay estimation increases.

6.2 Contributions of Thesis

Several contributions of this thesis include:

- A combined VBLAST decoding algorithm was introduced, which employs successive interference cancellation at the first step followed by parallel interference cancellation (PIC) as a second step. The performance of this combined scheme was investigated and it was verified that the combined scheme exploits both the advantages of ordering and of the PIC algorithm.
- A mathematical formulation for multi-user V-BLAST receivers operating in MIMO channels was developed.
- Linear and non-linear receiver structures were described for a VBLAST system with multiple asynchronous users. The performance of these receiver structures was evaluated using a simulation model. The receivers such as decorrelator, MMSE and MPIC receiver outperformed the matched filter receiver remarkably even in MIMO channels and it was

verified that the multiple antenna interference leads to the degradation of MPIC receiver performance.

- The effect of channel estimation error and delay estimation error were investigated for VBLAST receivers in both SISO and MIMO channels. It was observed that the performance of all receivers was very rapidly degraded as the error of time delay estimation becomes large and the performance of MPIC receiver highly depends on the accuracy of channel estimation.

6.3 Future Work

A few possible extensions to the work presented in this thesis are described below.

1 We considered block-based channel estimation techniques for investigating the effect of channel estimation error on a Rayleigh flat fading channel. For future work a frequency selective channel model might be considered. Moreover, both pilot-symbol-based and blind channel estimation techniques should be considered.

2 Another interesting extension is to investigate ways to share capacity on reverse link such as allocating higher data rates to stronger users. This scheme, known as multiuser diversity, we need to study the trade-off between throughput and fairness.

Bibliography

[1] S. M. Alamouti, “A simple transmit diversity technique for wireless communications,” IEEE Journal on Selected Areas in Communications, vol.16, pp. 1451~1458, October 1998.

[2] V. Tarokh, H. Jafarkhani, A. R. Calderbank, “Space-Time Block Coding for wireless communications: Performance Results,” IEEE Journal on Selected Areas in Communications, vol.17, pp.451~460, March 99.

[3] V.Tarokh, N. Sesahdri, A. R. Calderbank, “Space-Time codes for high data rate wireless communication :Performance criterion and code construction,” IEEE Transactions on Information Theory, vol.44, pp.744~765, March 1998.

[4] Gerard J. Foschini, “Layerd space-time architecture for wireless communications in a fading environment when using multi-element antennas,” Bell Labs Technical Journal, Autumn 1996.

[5] R. L. Peterson, R. E. Ziemer and D. E. Borth, *Introduction to spread spectrum communications*, Prentice Hall, 1995.

[6] S. Verdu, *Multiuser Detection*, Cambridge Univ. Press, 1998.

[7] R. M. Buehrer, N. S. Correal-Mendoza and B. D. Woerner, “A simulation comparison of multiuser receivers for cellular CDMA,” IEEE Transactions on Vehicular Technology, Vol. 49, No. 4, July 2000.

[8] R. Lupas and S. Verdu, “Linear multiuser detectors for synchronous code-division multiple-access channels,” IEEE Transactions Information Theory, Vol. 35, pp. 123~136, Jan.1989.

[9] M. K. Varanasi and B. Aazhang, “Multistage detection in asynchronous code-division multiple access communications,” IEEE Trans. Communication, Vol.38, pp.509~519, April 1990

[10] W. Wu and K. Chen, “Linear multiuser detectors for synchronous CDMA communication over rayleigh fading channels,” IEEE International Symposium, Personal, Indoor and Mobile Radio Communications, PIMRC'96, Seventh , vol. 2, pp. 578~582 Oct 1996.

[11] R. Kohno, M. Hatori and H. Imai, “Cancellation techniques of co-channel interference in asynchronous spread spectrum multiple access systems,” Electronics and Communication in Japan, vol.66-A, no.5, pp.20~29, 1983.

[12] N. S. Correal, R. M. Buehrer, and B. D. Woerner, “Improved CDMA performance through bias reduction for parallel interference cancellation,” IEEE International Symposium. Personal, Indoors and Mobile Radio Communication, pp. 565~569, 1997.

[13] John G. Proakis and Masoud Salehi, “Contemporary Communication Systems using Matlab,” Brooks/Cole, 2000.

[14] Gerard J. Foschini and Michael J. Gans, “On limits of wireless communications in a fading environment when using multiple antennas,” Wireless Personal Communications, 6, pp.311~335, March 1996.

[15] Gerard J. Foschini, “Layerd space-time architecture for wireless communications in a fading environment when using multi-element antennas,” Bell Labs Technical Journal, Autumn 1996.

[16] P. W. Wolniansky, G. J. Foschini, G. D. Golden, and R. A. Valenzuela, “V-BLAST : An architecture for realizing very high data rates over the rich-scattering wireless channel,” URSI International Symposium on Signals, Systems and Electronics, pp.295~300, 1998.

[17] G. D. Golden , G. J. Foschini, R. A. Valenzuela and P. W. Wolniansky, “ Detection algorithm and initial laboratory results using v-blast space-time communication architecture,” IEE Electronic Letters, Vol.35, No.1, pp.14~16, 7th January 1999.

[18] Stephan Baro, Gerhard Bauch, Aneta Pavlic and Andreas Semmler, “Improving BLAST performance using space-time block codes and turbo decoding,” GLOBECOM 2000, vol. 2, pp.1067~1071, 2000.

[19] M. Sellathurai and S. Haykin, “A simplified diagonal blast architecture with iterative parallel-interference cancelation receivers,” IEEE International Conference on Communications, vol. 10, pp.3067~3071, 2001.

[20] M. Sellathurai and S. Haykin, “Turbo-blast for high-speed wireless communications,” Wireless Communications and Networking Conference, vol.1, pp. 315~320, 2000.

[21] R. Gozali, “Space-time codes for high data rate wireless communications,” Ph.D. dissertation Virginia Polytechnic Institute and State University, 2002.

[22] H. Dai and A. F. Molisch, “Multiuser detection for interference-limited MIMO systems,” IEEE Vehicular Technology Conference 55th, vol.1, pp.45~49, spring 2002.

[23] R. L. Choi, R. D. Murch and K. B. Letaief, “MIMO CDMA antenna system for SINR enhancement,” IEEE Tranactions on Wireless Communications, vol. 2, no. 2, pp. 240~249, March 2003.

[24] D. Samardzija, P. Wolniansky and J. Ling, “Performance evaluation of the VBLAST algorithm in W-CDMA systems,” IEEE Vehicular Technology Conference, vol.2, pp.723~727, Fall 2001.

[25] J. G. Proakis, “Digital communications,” McGrawHill, Fourth edtion, 2000.

[26] Q. Sun, D. C. Cox, H. C. Huang and A. Lozano, “Estimation of continuous flat fading MIMO channels,” IEEE Trans. on Wireless Communications, vol.1, no.4 , pp.549~553, October 2002.

Vita

Mincheol Park was born in Korea, on May 25, 1973. He received his B.S. degree on Electronic Engineering from Inha University, Korea in 1996. He joined the M.S. program in Electrical & Computer Engineering at Virginia Polytechnic Institute and State University on August 2001. In Fall 2002, he became a member of Mobile and Portable Radio Research Group. His research interests include multi-user detection and space-time signal processing in MIMO systems.